THE EXPERIMENTAL RESULTS OF AN APPARATUS DESIGNED TO DETERMINE THE SPECIFIC ELECTRONIC CHARGE

Thesis by

John Irvin Lauritzen Jr.

In Partial Fulfillment of the Requirements

For the Degree of

Doctor of Philosophy

California Institute of Technology

Pasadena, California

1955

ACKNOWLEDGMENTS

The author wishes to express his deepest gratitude to Professor W. R. Smythe under whose direction the following work was done. His unstinting bestowal of time and advice was essential in the performance of this experiment. Deep appreciation is offered to my co-workers on this project, Dr. G. C. Dacey and Dr. W. T. Ogier. Dr. Ogier in particular has provided the author with important help and encouragement, even after he left this project and was occupied with his own endeavors. Much of the work has been a joint effort, where separation of contributions is impossible.

Advice and assistance has been given to this experiment by so many members of this laboratory that they cannot be enumerated. We are also indebted to the Office of Naval Research for providing the funds to execute this experiment.

ABSTRACT

An apparatus designed to measure the specific electronic charge fora free electron is described. A well collimated electron beam traverses axially a right circular cylindrical resonant cavity, which is operated so that the principal field interaction is due to a transverse, uniform, rotating magnetic field extending the length of the cavity. The cavity serves as a velocity selector so that the electron beam is undeflected, when it remains within the cavity an integral number of field cycles. The determination of (e/m_o) depends upon precise measurements of a length, a frequency, and a voltage. The holes, which provide the electron beam with access to the cavity, cause field distortion. The correction for this distortion is obtained empirically.

The experimental results obtained with this apparatus are stated. The failure to secure a significant determination of (e/m_o) is considered. The feasibility of a precise determination of (e/m_o) by the described method with certain important design changes is asserted.

TABLE OF CONTENTS

I. INTRODUCTORY DISCUSSION OF THE EXPERIMENT

1.0 Background of the Experiment

The most probable values of the fundamental atomic constants hold considerable interest for both the experimental and theoretical physicist. The interdependence of these constants implies that values obtained by utilizing all of the experimental evidence will have lower probable errors than values obtained from one or two particular experiments. The best method of obtaining these most probable values is by a least squares adjustment on an overdetermined set of equations containing the constants as variables and the unrelated individual experiments as input data.[1,2]

The improvement in our knowledge of the atomic constants is graphically illustrated by quoting the least-squares-adjusted value of the specific charge of the electron (e/m_o) obtained by Drs. Jesse W. M. DuMond and E. Richard Cohen in 1948[1]

$$(e/m_o) = (1.75936 \pm 0.00018) \times 10^7 \text{ emu/gr.}$$

and in 1953[2]

$$(e/m_o) = (1.75888 \pm 0.00005) \times 10^7 \text{ emu/gr.}$$

In addition to the reduction in the probable errors in this and other constants, the elimination of several pronounced inconsistencies was effected in this period. There remain, however, inconsistencies in the input data which are somewhat larger than would be expected from the quoted probable errors.

The input data in the least squares adjustment consist

of independent precision measurements of a relatively small number of atomic constants. Measurements of other constants have insufficient accuracy to possess appreciable weight in the calculations. A more extensive body of input data with confidence limits less than 100 parts per million is highly desirable. Dunnington performed the best direct measurement of the specific charge of unbound electrons in 1937 and obtained[3]

$$(e/m_o) = (1.7597 \pm 0.0004) \times 10^7 \text{ emu/gr.}$$

Since the error in this experiment is 230 ppm (parts per million), it is clear that a precise direct measurement of (e/m_o) would contribute to our knowledge of the fundamental atomic constants.

The probable effect of a precise determination of (e/m_o) will be better understood if we consider the best indirect measurement of this constant. By definition the Bohr Magneton, μ_o, and the proton gyromagnetic ratio, γ_p, are respectively

$$\mu_o = \tfrac{1}{2}(e/m_o)\,\bar{h}$$

$$\gamma_p = \tfrac{1}{2}(\mu_p/\bar{h}$$

where $\bar{h}$ is Planck's constant divided by 2π, and μ_p is the magnetic moment of the proton. Eliminating $\bar{h}$ we have

$$(e/m_o) = \gamma_p(\mu_o/\mu_p). \qquad (1)$$

An experiment on the Zeeman splitting in the ground state of hydrogen by Koenig, Prodell, and Kusch yields a highly accurate value of the magnetic moment of a bound electron in terms of the

proton magnetic moment in oil[4]

$$(\mu_s/\mu_p) = 658.2288 \pm 0.0006.$$

A more recent measurement by Beringer and Heald reinforces this value[5] $(\mu_s/\mu_p) = 658.2277 \pm 0002.$ The magnetic moment of a bound electron differs from one Bohr Magneton by two small relativistic terms. Calculations of Karplus and Kroll produce[6]

$$(\mu_s/\mu_o) = 1 + (\alpha/2\pi) - 2.973\,(\alpha/\pi)^2 \ldots = 1.0011453$$

Combining this result with (μ_s/μ_p) above we obtain

$$(\mu_o/\mu_p) = 657.4757 \pm 0.0006$$

The proton gyromagnetic ratio in oil has been determined by Thomas, Driscoll, and Hipple at the National Bureau of Standards[7]

$$\gamma_p = (2.67523 \pm 0.00006) \times 10^4 \text{ sec.}^{-1} \text{ gauss}^{-1}$$

Substituting these results into equation (1) we have

$$(e/m_o) = (1.75889 \pm 0.00004) \times 10^7 \text{ emu/gr.}$$

The error in this result is entirely due to the experiment of Thomas, Driscoll, and Hipple.

The highly precise knowledge of (μ_o/μ_p) and the form of equation (1) indicates a strong interdependence between the values accepted for γ_p and (e/m_o). Thus a direct determination of (e/m_o) with a probable error of better than a few parts in a hundred thousand will reduce the errors of the proton gyromagnetic ratio as well as the specific charge of the electron when used as an input datum in

a least squares adjustment.

The experiment described in this paper was undertaken to obtain an accurate value of (e/m_o). While this goal was not achieved, the author believes that the method can produce a useful result if certain modifications in the instrumentation are effected. Therefore, this paper will describe the apparatus, develop the theory of the experiment, summarize and analyze the results, and finally consider the alterations required for the method to furnish useful data.

1.1 Introductory Description of Method

A direct velocity measurement of the specific charge of the electron requires that electrons be accelerated through a known voltage, V, and that their velocity, v, be measured. (e/m_o) is obtained by application of the energy equation

$$(e/m_o)V = c^2\left\{\left[1-(v/c)^2\right]^{-\frac{1}{2}} - 1\right\} = v^2/2\left\{1+\frac{3}{4}(v/c)^2\ldots\right\} \quad (1)$$

where c, the velocity of light, is known to better than 10 ppm. If $(v/c) \lesssim 0.1$, (e/m_o) is independent of c experimentally within 1 ppm.

The device used to measure velocities in this experiment is a radio frequency resonant cavity shaped as a right circular cylinder. The electron trajectories are along the cavity axis, and the cavity is operated so that the electrons experience a magnetic field of constant magnitude normal to the cavity axis and rotating about the axis at the cavity frequency. Assuming that the electron velocity along the cavity axis is constant, the force vector has a magnitude eBv and rotates at the cavity frequency in a plane normal

to the axis. The electrons will be deflected by the cavity fields through an angle θ, which is the ratio of the change in transverse velocity to the axial velocity v. Under our assumptions the deflection is

$$\theta = (e/m_o)\,(B/\pi f)\,\left[1-(v/c)^2\right]^{\frac{1}{2}}\,\left|\sin(\pi fd/v)\right| \qquad (2)$$

where d and f are the cavity length and frequency respectively. The direction in which the electrons are deflected through an angle θ depends upon their phase of entry into the cavity. Then a continuous electron beam will be spread into a cone of half angle θ.

If the time of transit of the electron through the cavity is an integral multiple of the cavity period, there is no deflection since the effect of the rotating force vector cancels over each complete cycle. Then $v = (fd/k)$, where k is an integer, and the corresponding accelerating voltage, V_k, is called a "resonant" voltage. In this experiment the length and frequency of the cavity are maintained constant, while the accelerating voltage is varied over a small range of values about the "resonant" voltage, and V_k is obtained by interpolation from the resulting electron deflections. If two such "resonant" voltages, V_k and V_n, corresponding to velocities (fd/k) and (fd/n), are substituted in equation (1), the specific charge of the electron is given by

$$(e/m_o) = \frac{(fd)^2}{2(V_k-V_n)}\,(k^{-2}-n^{-2})\left\{1+\frac{3}{4}\,(fd)^2c^{-2}(k^{-2}+n^{-2})..\right\} \qquad (3)$$

This equation was derived for an idealized field configuration and electron interaction, but the main characteristics are unchanged when the appropriate corrections are made. An accurate

determination of (e/m_o) requires a precision measurement of three experimental quantities: a length, a frequency, and a voltage. Standards for these quantities are readily available, and comparisons are easily performed so that the limitation of accuracy from this source is no more than 10 ppm due to uncertainties in the voltage standard.

Certain difficulties characteristically appear in a direct velocity measurement of (e/m_o). First the energy actually delivered to the electrons at the cathode is uncertain due to contact potentials, thermal electron potentials, surface work functions, and space charge effects. This is avoided in this experiment since the voltage appears in equation (3) in the form $(V_k - V_n)$. Then if the conditions surrounding the cathode remain constant independent of the accelerating potential, the uncertainties are canceled. Second the field configuration used to determine the electron velocities is difficult to ascertain precisely. This problem will be discussed in Chapter 3. Third the resolution in the deflection determination of velocities is low and this will be considered below.

In this experiment the frequency is fixed by the radius of the cavity at $f = 2.62\ 10^9\ (\text{sec.})^{-1}$. Two sets of "resonant" voltages were obtained with $d = 1.20"$ and $d = 1.63"$. With $d = 1.20"$ the "resonant" voltages were 2043, 1143, and 729 volts corresponding to $k = 3$, 4, and 5 respectively. With $d = 1.63"$ the "resonant" voltages were 2130, 1357, and 940 volts corresponding to $k = 4$, 5, and 6 respectively. Since the voltage differences between "resonant" voltages is on the order of 1000 volts, these voltages must be determined to 0.01 volts to obtain an accuracy of 10 ppm.

When the accelerating voltage is near a "resonant" voltage

$$V = V_k + \Delta V; \quad v = (fd/k) + \Delta v; \quad \Delta v/v = \tfrac{1}{2}\Delta V/V_k$$

Substitution into equation (2) yields after a first order expansion

$$\theta = \tfrac{1}{2}(e/m_o)\,(Bk/f)\; V/V_k$$

The value of the magnetic field intensity is limited to about 5 gauss by the R. F. power supply. Then for a typical "resonant" voltage

$$(d\theta/dV) = 6\ 10^{-5}. \quad B = 5 \text{ gauss}; \; k = 4; \; V = 1143 \text{ volts}.$$

Then an angular deflection of about 10^{-6} radians must be resolved in order to obtain an accuracy of about 20 ppm. To obtain such resolution the electron beam must be collimated to as small a diameter as possible, and the distance traveled by the electron beam must be as large as possible. The electron beam travels about eight feet before falling upon the electron detector. The cavity is situated near the midpoint of the path, 50 inches from the detector. Then a deflection somewhat less than 10^{-4} cm. at the detector must be resolved. This is possible only when the stability of all factors is optimum. The diameter of the electron beam is .008 inches at the detector since it is collimated by a .002" pinhole at the electron source and a .004 inches pinhole just beyond the cavity.

Since the electrons travel eight feet the magnetic shielding must be excellent. The radius of curvature of a 2000 volt electron in the earth's magnetic field is about 10 feet so that the electrons will not pass through the instrument without good shielding. All unstable magnetic fields must be eliminated entirely for beam

stability. It is also necessary for beam stability to operate the electron beam at the lowest intensity compatible with detector sensitivity in order to minimize the formation of positive ions from residual gas and to reduce the charging of surfaces.

An important correction will be mentioned here. The electron beam has access to the resonant cavity through two accurately centered holes in the flat end surfaces of the cavity. The cavity fields penetrate these holes so that the effective length of the cavity is increased by a few per cent and the deflection sensitivity is appreciably decreased. This correction will be discussed in the next section and in Chapter 2 after the theory of the cavity fields is amplified.

1.2 Introductory Description of Apparatus

The apparatus will be described in detail in a later chapter. A brief discussion of the relationship between the various parts will be presented here with emphasis on those points necessary to clarify the theory of the method.

The electron beam traverses about eight feet from the electron gun to the current collector through a region evacuated by a silicone oil diffusion pump. The electron beam is magnetically and electrically shielded. Approximately midway between the gun and the collector lies a right circular cylindrical resonant cavity with its axis aligned with the trajectory of the electrons. The electron beam has access to the cavity through two circular holes .090 inches in diameter centered in the flat end surfaces of the cavity about its axis. Two probes to the cylindrical sur-

face of the cavity supply the R.F. power to excite the cavity fields. The electron gun, electron collector, and resonant cavity are supported by the aluminum vacuum envelope.

The electron beam leaves the electron gun fully accelerated through a circular pinhole .002 inches in diameter. The accelerating voltage of the beam may be varied between 700 and 2200 volts, while the cathode conditions remain unchanged. No focusing fields are applied to the electron beam after it leaves the electron gun. The beam is collimated geometrically by the electron gun pinhole and a circular pinhole .004 inches in diameter just beyond the cavity. Then the electron beam has a diameter of about .008 inches when it falls upon the electron collector.

The electron beam is collected in a Faraday cup after passing through a circular pinhole .008 inches in diameter. The current collected is amplified and recorded on a 50 cm. scale by a galvanometer. The current collected through the .008 inches pinhole is used as a measure of the deflection of the electron beam. For simplicity let us suppose that the electron beam has a uniform density with exactly the radius of the collector pinhole. Then the current received is a maximum when the electron beam is centered on the pinhole. If the center of the electron beam is displaced a distance D from the center of the pinhole, the current collected is

$$I = I_o \left\{ \frac{2}{\pi} \cos^{-1} \left(\frac{D}{2R}\right) - \frac{D\sqrt{4R^2 - D^2}}{2\pi R^2} \right\} \qquad (1)$$

where R is the radius of the pinhole, and I_o the current when D = 0.

The corresponding rate of change of current is

$$\frac{dI}{dD} = -\frac{2I_o}{\pi R^2}\sqrt{4R^2-D^2} \qquad (2)$$

Thus the current received is a maximum when the beam is centered and as the beam is deflected the current falls off at a rate that is approximately constant when D is small.

In the last section it was seen that the beam when not at a resonant voltage was deflected through an angle ϕ by the cavity. The direction of the deflection rotates with the cavity fields. If the distance from the cavity to the collector is L, the beam is instantaneously deflected by a distance $D = \phi L$. The beam then rotates about the center of the pinhole at the cavity frequency when the beam is properly centered. The intersectional area of the pinhole and beam area remain constant however during this rotation so that equations (1) and (2) apply with ϕL substituted for D.

If the accelerating voltage of the electron beam is varied in the vicinity of the resonant voltage, a current "resonance" peak will be measured as plotted against the voltage. The sides of this peak are used to interpolate the "resonant" voltage.

The remainder of the apparatus is external to the instrument and consists of power supplies which furnish the R.F. and electron gun power, and measuring devices to determine the accelerating voltage and cavity frequency continuously during deflection measurements.

1.3 Introductory Description of Theory of the Experiment

The vector potential in cylindrical coordinates ρ, ϕ, z for a right circular cylindrical cavity excited in the TM_{110} mode is[8]

$$A_z = (2Bc/\omega)J_1(\omega\rho/c)\sin(\phi+\delta)\cos(\omega t+\psi);\quad (\omega b/c)=3.8317$$

where ω and b are the angular frequency and radius of the cavity, B is the field intensity on the axis, and c is the velocity of light. In this experiment two such modes, nearly orthogonal in space and time, are excited. Dr. Ogier has shown that in this case the vector potential for a perfect cavity may be represented by[9]

$$A_z=(2c/\omega)J_1(\omega\rho/c)\left\{B_1\sin\phi\cos(\omega t)-B_2\cos\phi\sin(\omega t)\right\} \qquad (1)$$

From this expression the fields near the cavity axis are

$$B_x=B_1\cos(\omega t)-(\omega^2/8c^2)\left\{B_1(x^2+3y^2)\cos\omega t-2xyB_2\sin\omega t\right\}+\ldots \qquad (2)$$

$$B_y=B_2\sin(\omega t)-(\omega^2/8c^2)\left\{B_2(3x^2+y^2)\sin\omega t-2xyB_1\cos\omega t\right\}+\ldots \qquad (3)$$

$$E_z=-\omega\left\{B_1y\sin\omega t+B_2x\cos\omega t\right\}+\ldots;\ B_z=E_x=E_y=0 \qquad (4)$$

All neglected terms are of order $(\omega\rho/c)^3$ or higher. The fields are independent of z and extend from z = 0 to z = d, the entire cavity length.

Dr. Dacey has obtained the equations of motion for an electron in these fields assuming that the trajectory of the electron is so close to the cavity axis that all terms dependent on x and y are negligible and that $B_1 = B_2 = B$.[10]

With the initial conditions

$$\dot{z} = v; \quad \dot{x} = \dot{y} = 0; \quad Z = 0 \text{ at } t = 0$$

he obtained the solutions

$$\dot{x} = (2bv/k)\sin(kt/2)\left\{(\omega/k)\cos(\omega t)\sin(kt/2) - \sin(\omega t)\cos(kt/2)\right\} \tag{5}$$

$$\dot{y} = -(2bv/k)\sin(kt/2)\left\{(\omega/k)\sin(\omega t)\sin(kt/2) - \cos(\omega t)\cos(kt/2)\right\} \tag{6}$$

$$\dot{z} = v\left\{(\omega/k)^2 + (b/k)^2\cos(kt)\right\} \tag{7}$$

where $b = |(e/m_o)|\, B\left\{1-(v/c)^2\right\}^{\frac{1}{2}}$ and $k^2 = \omega^2 + b^2$. The time of transit for the electron to traverse the cavity is obtained from equation (7)

$$\int_o^d dz = d = \int_o^\tau \dot{z}dt = v\left\{(\omega/k)^2\tau + (b^2/k^3)\sin(k\tau)\right\} \tag{8}$$

The transverse velocity of the electron is obtained directly from equations (5) and (6) by substituting $t = \tau$.

$$\left\{\dot{x}^2 + \dot{y}^2\right\}^{\frac{1}{2}} = (2b\omega v/k^2)\ |\sin(k\tau/2)|\ \left\{1 + (b/\omega)^2\cos^2(k\tau/2)\right\}^{\frac{1}{2}} \tag{9}$$

It follows immediately that the electron is undeflected when $k = 2n\pi$. Substituting into equation (8) we have

$$v_n = (fd/n)\left\{1 + (b/\omega)^2\right\}^{\frac{3}{2}} \tag{10}$$

(e/m_o) is obtained by the substitution of this value of the velocity into the energy relationship. This expression for (e/m_o) differs from that given in 1.2 by the correction factor $\left\{1+(b/\omega)^2\right\}^3$. The field intensity B is limited by the R.F. power supply so that

$b/\omega \leqslant 5\ 10^{-3}$. Then the change in the value of (e/m_o) is less than 80 ppm.

The angle through which an electron is deflected by the cavity is given by

$$\theta = \left[\dot{x}^2+\dot{y}^2\right]^{\frac{1}{2}}/\dot{z} = (2b/\omega)\left|\sin(k\tau/2)\right| \frac{\left\{1+(b/\omega)^2\cos^2(k\tau/2)\right\}^{\frac{1}{2}}}{1+(b/\omega)^2\cos(k\tau)} \qquad (11)$$

where $k\tau = (k^3d/\omega^2v) - (b/k)^2 \sin(k^3d/\omega^2v) \ \ldots$

Expanding we have within 40 ppm

$$\theta = (2b/\omega)\left|\sin\left\{(\omega d/2v)\ (1+b^2/\omega^2)^{\frac{3}{2}}\right\}\right| \qquad (12)$$

If this result is compared to equation 1.1 (2) it is seen that no startling change has occurred. The sensitivity at resonance is when $(\omega d/2v) \approx n\pi$

$$(d\theta/dV) = \tfrac{1}{2}(d\theta/dv)(v/V) \approx (n\pi b/\omega V) \qquad (13)$$

The sensitivity obtained here is identical with that found in Section 1.1. Investigation of equations (5) and (6) shows that the deflection is essentially at right angles to the orientation of the magnetic field when the electron entered the cavity, i.e. the x component of velocity is nearly stationary near the "resonant" velocity.

The geometrical trajectories of the electrons are obtained by integrating equations (5) and (6) above. If the results are expanded in powers of $(b/\omega)^2$ we have

$$x-x(z=0) = -(bv/k^2)\left\{kt-\sin(kt)\right\} + \ldots \qquad (14)$$

$$y-y(z=0) = (bv/k^2)\left\{1-\cos(kt)\right\} + \ldots \qquad (15)$$

The neglected terms are less than 15 Ångströms in all cases and are negligible for the accuracy required. It is seen that the electrons follow a cycloidal path in this perfect cavity. Since the collimating pinhole is located on the cavity axis at the exit from the cavity it follows that $x(z=d)^2+y(z=d)^2 \ll (.002")^2$. If $x(z=d)=y(z=d)=0$, when $k\tau = 2n\pi$

$$x(z=0) = (b\omega/k^2)d \; ; \qquad y(z=0) = 0 \tag{16}$$

Then only those electrons which fall within a circle of radius .002 inches about a point $(b\omega/k^2)d$ from the cavity center in the direction which the magnetic field points when the electron enters the cavity. If B=5 gauss then $(b\omega/k^2)d$ equals .006" and .008" when d is 1.2 and 1.6 inches respectively. Then as the magnetic field rotates the electrons are selected from a ring of about .012" to .016" in diameter. This displacement has several important consequences.

First if an electron enters the cavity with a "resonant" velocity along the z axis the electron will be essentially undeflected by the cavity. Since the electrons originate at a point source those that leave the exit pinhole of the cavity have a transverse velocity spread that accounts for the diameter of the selection ring in the four foot distance between electron gun and cavity. Since the distance between the cavity and the collector is also four feet, the electron beam at the collector has the shape of a ring with the diameter of the selected ring at the cavity entrance. Then the current collected through the collector pinhole is less at "resonance" with the R.F. on than it is with no cavity fields. It should be noted

that no shift in the resonance velocity occurs but only a decrease in resolution, because the transverse velocity for a given electron is in the x component which is almost stationary near the "resonant" velocity.

The second important effect of the electron displacement is that the "resonant" velocity is changed due to the electron interaction with the electric fields of the cavity. The electron enters the cavity at a distance of .006" to .008" from the axis where the potential drop across the cavity is 36 to 60 volts which is not negligible. If the first order electric field terms are included in the equations of motion for a perfect cavity, the velocities and displacements may be obtained in closed form. The expressions are complicated, however, and do not give much insight into the interaction. For this reason the electric field interaction will be considered in Chapter 3, and the results only mentioned here. The deflection sensitivity and the electron displacement are essentially unchanged, but the resonance velocity is changed so that

$$v_n=(fd/n)\left\{1+(21/4)(b/\omega)^2 \ \ldots \right\} \tag{17}$$

Comparison with equation (10) above shows that the electric field interaction causes a shift of almost 200 ppm in (e/m_o). The contribution of the second order magnetic field terms is negligible, however.

The expressions above derived from the fields of a perfect cavity furnish the general behavior of an electron in this experiment. The corrections required for the end holes in the cavity will be discussed in detail in Chapter 3. A brief discussion of the

effect of the end holes is necessary for an understanding of the experimental procedure.

The fields of the cavity penetrate the end holes instead of starting at the walls of the cavity. If the origin is taken at the center of the cavity the fields on the cavity axis have the form

$$B_x = B_1 F(z)\cos(\omega t) \quad ; \quad B_y = B_2 F(z)\sin(\omega t)$$

where $F(0)=1$, $F(-\infty)=0$, and $F(z)=F(-z)$. Dr. Ogier has shown that the deflection due to the cavity is nearly

$$\theta = 2b(T)/\omega \int_{-\infty}^{o} F(z)\cos(\omega z/v)\,d(\omega z/v) \tag{18}$$

where $b(T) = (|e|/m_o)\left\{1-(v/c)^2\right\}^{\frac{1}{2}}(B_1^2\cos^2\omega T + B_2^2\sin^2\omega T)^{\frac{1}{2}}$.

where T is the time when the electron is at z = 0.

The form of b(T) shows that the beam is deflected by the cavity into an elliptical cone instead of a circular cone if the fields are not circularly polarized. Of more importance is the fact that the "resonant" velocity is not shifted if the two modes have unequal intensity. Within the order of $(b/\omega)^2$ the condition of resonance is that

$$\int_{-\infty}^{o} F(z)\cos(\omega z/v)\,d(\omega z/v) = 0 \tag{19}$$

F(z) is independent of ω and v, but contains d implicitly. The solutions of this integral equation have the form

$$(\omega/v)\left\{d+\Delta d(v)\right\} = 2n\pi \qquad n\ 1, 2, 3, \ldots \tag{20}$$

The magnitude of $\Delta d(v)$ results in a difference of v of less than two

per cent. In addition $\Delta d(v)$ is almost independent of v so that over the velocity range used in this experiment $\{\Delta d(v)/d\}$ varies only a few parts in ten thousand. $\Delta d(v)$ is independent of the magnetic field intensities B_1 and B_2 from its definition. Actually the dependence is slight and may be included if we write the "resonant velocities in the form

$$v = (f/n)\left\{d+\Delta d(v)\right\}\left\{1+a(v)(b/\omega)^2 \ \ldots\right\} \tag{21}$$

for the circularly polarized case where $b=(|e|B/m_o)$.

Since $\Delta d(v)$ is but slightly dependent on v, $\Delta d(v)$ may be obtained empirically. If two sets of resonances are obtained for two different cavity lengths d_1 and d_2, the various energy relationships may be solved for $\Delta d(v)$, and then resubstituting this value of $\Delta d(v)$, (e/m_o) is obtained. The theory of this empirical determination of Δd will be discussed in greater detail in Chapter 3 , but it should be mentioned that this theory fails if any static electric fields are present in the cavity.

1.4 Brief Summary of Results

The value of (e/m_o) is obtained from the equation

$$(e/m_o)=\tfrac{1}{2}(V_k-V_n)^{-1}(v_k^2-v_n^2)\left\{1+\frac{3}{4}(v_k^2+v_n^2)c^{-2}+\ldots\right\}$$

where $v_k=fk^{-1}\left\{d+\Delta d(v_k)\right\}$; $v_n=f_n^{-1}\left\{d+\Delta d(v_n)\right\}$; k, n integers.

To obtain $\Delta d(v)$ we must measure the "resonant" voltages for two separate cavity lengths d_1 and d_2. The experimental data in this experiment may thus be summarized (neglecting the magnetic field strength)

d	1.1954 inches	1.6295 inches
f	$2.6200\ 10^{9}$ sec.$^{-1}$	$2.6200\ 10^{9}$ sec.$^{-1}$
V(n=3) - V(n=4)	899.50 0.07 volts	
V(n=4) - V(n=5)	414.58 0.09 volts	772.44 0.09 volts
V(n=5) - V(n=6)		416.83 0.06 volts
V(n=3)	2043.06 0.07 volts	
V(n=6)		940.48 0.03 volts

The uncertainty of d and f is in the last place, and these errors may be reduced if it is desirable. The "resonant" voltage is obtained by interpolation from the straight sides of the plot of electron beam current collected against the accelerating voltage applied to the beam. These plots, which are called current peaks, will be discussed in a later chapter. The intersection of a single well formed peak is certain to within a few hundredths of a volt. The measured intersections vary by as much as several tenths of a volt when good stability is attained. If the fluctuations are random, probability theory may be applied, and the errors in "resonant" voltage quoted above are the standard errors under this assumption.

The "resonant" voltages are then known to within 0.1 volts, but are ineffectual in determining (e/m_o). This is illustrated if we solve for $\Delta d(v)$ for the six "resonant" voltages, assuming that the contact potentials in the electron gun are zero and that $(e/m_o) = 1.75888\ 10^{7}$ emu/gr. Tabulating $\Delta d(v)$

	d 1.1954 inches	d 1.6295 inches
n=3	0.0241 cm.	
n=4	0.0205 cm.	0.0269 cm.
n=5	0.0162 cm.	0.0229 cm.
n=6		0.0208 cm.

While the values of $\Delta d(v)$ quoted above depend on many factors, it will be seen in Chapter 4 that a basic inconsistency prevents an accurate determination of (e/m_o).

1.5 History of the Experiment

At the end of World War II (e/m_o) was known less accurately than any other important fundamental constant. In 1947 Dr. W. R. Smythe requested Dr. C. R. Wilts, then a graduate student at this laboratory, to investigate a direct velocity measurement of (e/m_o) using microwave techniques. Concluding that the electron velocity could be accurately measured by magnetic deflection in a resonant cavity, Dr. Wilts successfully performed a preliminary measurement.[11]

Under the supervision of Dr. Smythe three graduate students at this laboratory have participated in this experiment: Dr. George C. Dacey, Dr. Walter T. Ogier, and the author. In 1948 Dr. Dacey produced the basic design of the apparatus which augmented the design of Dr. Wilts with necessary refinements. Construction of the apparatus was under way in 1949 when Dr. Ogier joined the project, and was essentially complete in 1950 when the author joined the project, assuming responsibility for the voltage measurement

and collection and interpretation of data.

The difficulties of forming an electron beam suitable for a precision measurement had been underestimated. Dr. Dacey left the project in 1951 after demonstrating the possibility of a precision measurement, but it was not until the fall of 1952 that a suitable electron gun was developed. In 1953 Dr. Ogier left the project after establishing that the resolution of the instrument was sufficient for a significant measurement, but he has continued to contribute valuable aid and advice since that time.

In the next year the author with the extensive help of Dr. Smythe improved the stability of all elements until significant measurements were possible. In addition an important asymmetry in the resonant cavity was corrected. Finally in the latter part of 1954 sufficient precise data were collected to terminate the experiment.

II. DESCRIPTION OF THE APPARATUS

2.0 General Description of the Instrument

The mechanical structure has been discussed in detail by Dr. G. C. Dacey[10] and Dr. W. T. Ogier[9]. A short discussion will be given here as an aid in visualizing the instrument. The instrument is schematically drawn in Fig. 1, and the numbers appearing in parentheses in the text refer to the numbers in the drawing.

The aluminum vacuum header (1) is bolted to a brass plate on a wooden support. To the vacuum header are bolted a massive brass ring (2) and an auxiliary mounting ring (3). The brass ring supports the resonant cavity (4) and contains radial passages for R. F. power inputs (6) and cooling water (7) and longitudinal passages for vacuum pumping (5). This central section supports the remainder of the instrument.

Two aluminum tubes (8), which are four feet long, four inches in diameter, and flanged at both ends, are cantilevered from the vacuum header and auxiliary rings. The electron gun (9) and the collector end plate (10) are mounted at the end of these tubes. The entire system is evacuated, and all seals are made with "O" rings.

The system is evacuated by an oil diffusion pump supported directly below the vacuum header by a cold trapped column. The electron gun is separately evacuated by a 100 liter/sec. oil diffusion pump connected to the small vacuum header (11) by a cold trapped column. A pulley and counterweight mounted on the wooden frame compensates for the weight of the electron gun pumping system.

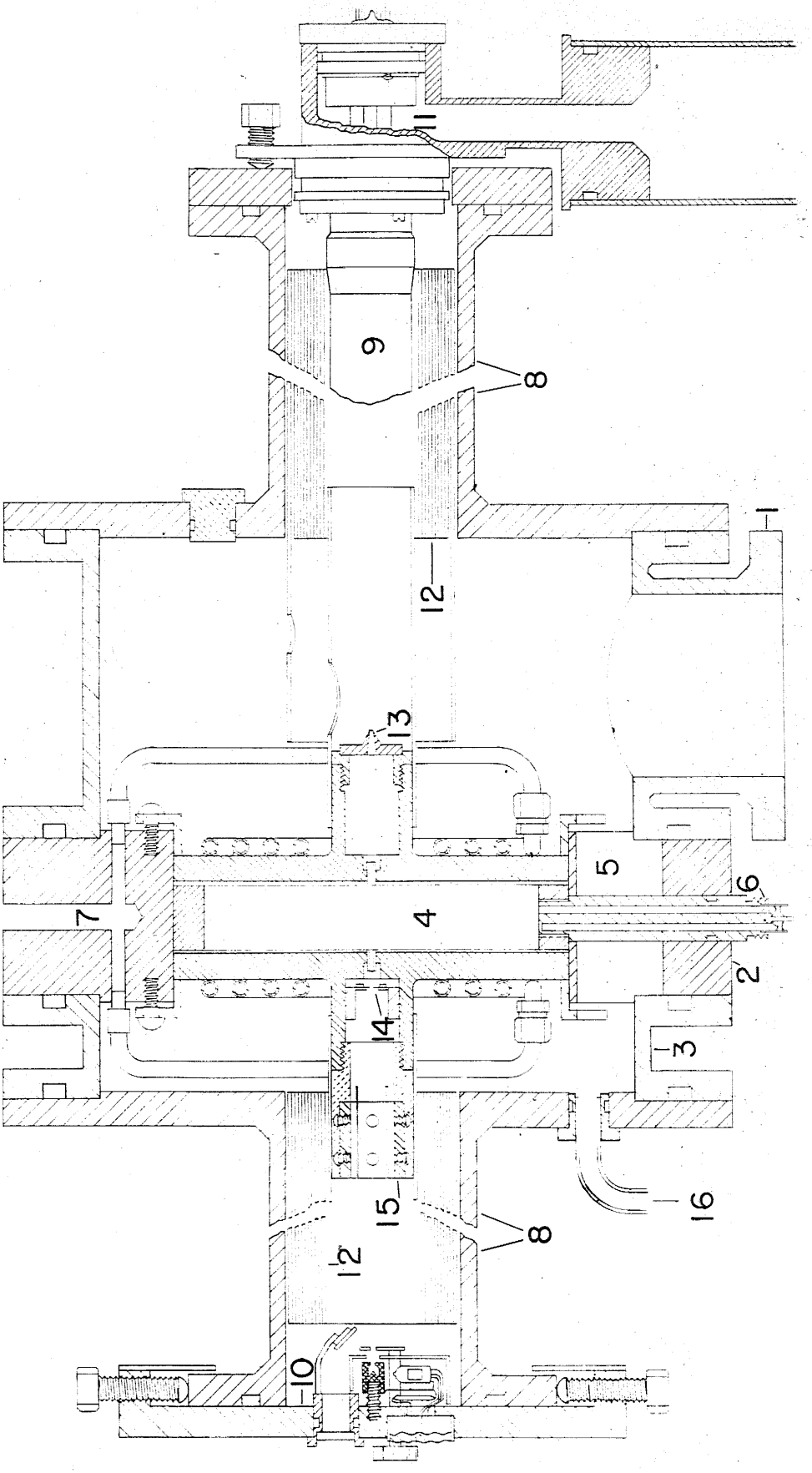

FIG. I. SCHEMATIC DRAWING OF THE INSTRUMENT

C.I.T. O.N.R. PHYSICS 18

The electron gun may be aimed mechanically by the means of three bolts. The collector end plate may be moved by the use of four bolts so that the current collector is aligned by the beam. To shield the electron beam passing through the long tubes, nests of three mu-metal and three copper shields are included in the tube (12). Magnetic shielding in the central region is achieved by small mu-metal cylinders at the ends of the cavity and larger mu-metal shields mounted both exteriorly and interiorly.

On both sides of the cavity collimating holes are located; the hole preceding the cavity (13) is 1/16" and prevents the electron beam from falling directly upon any cavity surface, and the pinhole following the cavity (14) is .004" and provides the final collimation. Both holes are mounted so that they lie on the cavity axis. Just beyond the .004" pinhole an electrostatic deflector (15) is mounted.

2.1 Construction of Resonant Cavity

The shape of the resonant cavity is a right circular cylinder. The two plane surfaces are formed by 1/2" copper plates which have been plated with about .020" of chromium and then ground optically flat. Soft copper tubing has been soldered on the reverse side of these plates in order that they may be water cooled. The cylindrical surface is formed by one or two sintered molybdenum rings. The inner and outer cylindrical surfaces of these rings have been accurately machined to 5.487" and 6.500". The flat surfaces of these rings have been ground flat and parallel. The principal ring is 1.1954" long and is flat and parallel within

.00001". The length of the cavity is increased by adding an auxiliary ring that is .4341" long and flat and parallel within .00008". Four symmetrically spaced 5/8" holes were drilled in the principal molybdenum ring to provide access for R. F. power.

The outer diameters of the molybdenum rings and end plates and the inner diameter of the massive brass ring that supports them has been machined to 6.500" with precision. The play is certainly less than .001". This snug fit prevents an appreciable tilt of the cavity axis. The position of the large molybdenum ring is determined by the four input probes extending through the brass ring into the four holes in the cavity wall. Pressure rings bearing on the outer edge of the end plates hold the cavity together.

It is necessary that the contact between the molybdenum rings and the endplates be excellent. It has been found that the Q of the cavity is drastically affected by this contact. The high experimental Q is taken as evidence that these contacts are good.

Copper tubes pass through the brass ring and are sealed to the cooling coils on the end plates by Imperial fittings. Great care is taken to insure that no strain is placed on the endplates. The temperature of the cooling water is measured by a thermometer after it leaves the cavity. The water pressure is constant on any given day but varies over a period of time. A typical flow rate is 28 cc per second. The observed temperature rise of this water due to R. F. power dissipation is $0.8^{\circ}C$ corresponding to 95 watts.

Circular holes accurately centered in the endplate must be present to allow the electron beam to pass along the axis of the cavity. As originally constructed these holes were believed to be

.125" in diameter, normal to the chromium surface, and precisely centered. A defect of these holes was that the edges were not precisely defined due to very fine cracks in the chromium extending radially outward. Chips of chromium with dimensions on the order of .001" were missing where the radial lines intercepted the edge of the holes. Another defect of these holes was that static electric fields due to the contact potential between the chromium and the copper existed in regions where the R. F. fields were not negligible. Theoretical prediction of the combined interaction of these fields upon electrons is difficult to calculate. Both of these defects could be corrected by inserting chromium bushings with accurately known dimensions and precise edges into these holes.

The bushings were constructed by plating chromium on iron rods machined to a known dimension. While still centered by the iron rod, the chromium was ground and polished to the desired size and shape. The rod was then cut off with a diamond saw, and the iron was dissolved out with hydrochloric acid. This left a cylindrical bushing of inner diameter .0899" and the correct outer diameter to be press fitted into the cavity holes. The length of these bushings was 3/8" and the outer surface of that part not presented to the cavity was slightly tapered so that the bushings could be press fitted more easily. The edges on these bushings are excellent.

It was discovered during the installation of these bushings that the existing 1/8" holes were as much as .005" off the center of the end plates and deviated appreciably from the normal to the chromium surfaces. It was essential to have these holes centered and normal to the surface. The holes were reamed from the

reverse side so that only a depth of 1/8" of the hole remained to be ground. This hole was ground on a precision lathe and it is believed to be centered to .0001" and accurately normal to the face of the end plate. Unfortunately, the grinding process caused the chromium surface about the re-centered holes to rise slightly so that the surface surrounding the holes is conical rather than flat extending a distance of somewhat more than 1/8". The height of the rise on the end plates nearest to and farthest from the electron gun is .0001" and .0005" respectively.

The chromium bushings were then press fitted into these holes until flush with the edges of the holes. The small cracks surrounding these bushings were packed with graphite so that the R.F. current of the cavity would be readily conducted across the cracks.

2.2 The Cavity Power Supply and Frequency Measuring Equipment

The radio frequency power supply has been discussed in great detail by Dr. W. T. Ogier. Readers are referred to his thesis for a close description. The cavity power for each mode is furnished by a Sperry Type XZF-8529 klystron. Both of these power klystrons are driven by a Sperry Type SRL-6 klystron through a power and phase splitting system. This project is indebted to Sperry Gyroscope Co., Inc., for furnishing these klystrons, which are pre-production models produced as part of a klystron development program.

The Sperry SRL-6 klystron is operated with the case grounded, the cathode at 1000 volts negative, the reflector about 200 volts negative with respect to the cathode, and with a beam current of 175 ma. The reflector voltage which is the important determinant of the

oscillation frequency may be varied over a range of 15 volts, and the corresponding frequency variation is greater than the acceptance band of the resonant cavity. The cavity of the klystron is of the bellows type and has been tuned for maximum power delivered to the resonant cavity. The noise band output of the klystron has been reduced to 20 kilocycles by immersing the klystron in a water-cooled oil bath and by heating the filament with a storage battery. After complete warm-up the drift of the klystron is slight. The output of the SRL-6 is transmitted by a 50 ohm coaxial line through an attenuator pad to a type "T" power and phase splitter which feeds the divided power into the type 8529 klystrons.

These are double cavity, cascade type klystrons, cooled both by water and air, and tunable by rotating paddles. The disk cathodes are indirectly heated with a bombarding beam dissipating about 100 watts. The cavity beam is about 200 ma at 2500 volts. The output of these klystrons is transmitted to the cavity input probes through about one foot of rectangular waveguide and three feet of flexible, 50 ohm impedance, high power coaxial line. The cavity input probes pass through the upper holes in the molybdenum ring and are magnetically coupled to the cavity by broad flat loops projected slightly into the cavity. In this way the cavity receives about 50 watts of power in each mode.

In the holes in the molybdenum ring opposite the cavity input loops are located two brass plugs which may be adjusted so that the two modes operate at the same resonant frequency. In these plugs are very small loops that receive R. F. signals from the cavity fields. These signals are presented to a microammeter

through crystal rectifiers. The meter readings are measures of the field intensity in the resonant cavity, and they are used both to tune the R. F. equipment and to monitor the R. F. fields during peak measurements.

The frequency measuring equipment is thoroughly discussed in the thesis of Dr. W. T. Ogier. The standard of comparison is a standard one megacycle crystal accurate to 20 ppm. The 2610th harmonic of this crystal is obtained by direct frequency multiplication in electronic amplifier stages. A small amount of R. F. power is obtained from one power klystron from a slot in the rectangular wave guide, and this signal is fed into a mixer with the 2610 megacycle signal. The beat frequency is continuously monitored by a Navy type RBH short wave receiver, manufactured by Scott Radio Laboratories. This radio has a 5 kilocycle pass band, and the klystron noise output is distinctly audible when all R. F. contacts are good. The beat frequency may be read directly off the remarkably accurate dial.

The 2610 megacycle signal has some 1 megacycle modulation causing the beat frequency signal to have side bands at a one megacycle distance. An independent frequency check has been made by coupling an accurate coaxial type wave meter into the wave guide. This wave meter has an accuracy $\pm$ .5 megacycles. The cavity frequency therefore is near 2620 megacycles.

2.3 Electron Gun and its Power Supplies

The electron gun used in this experiment, Fig. 2, is separately pumped and cold-trapped, and is, therefore, mounted on

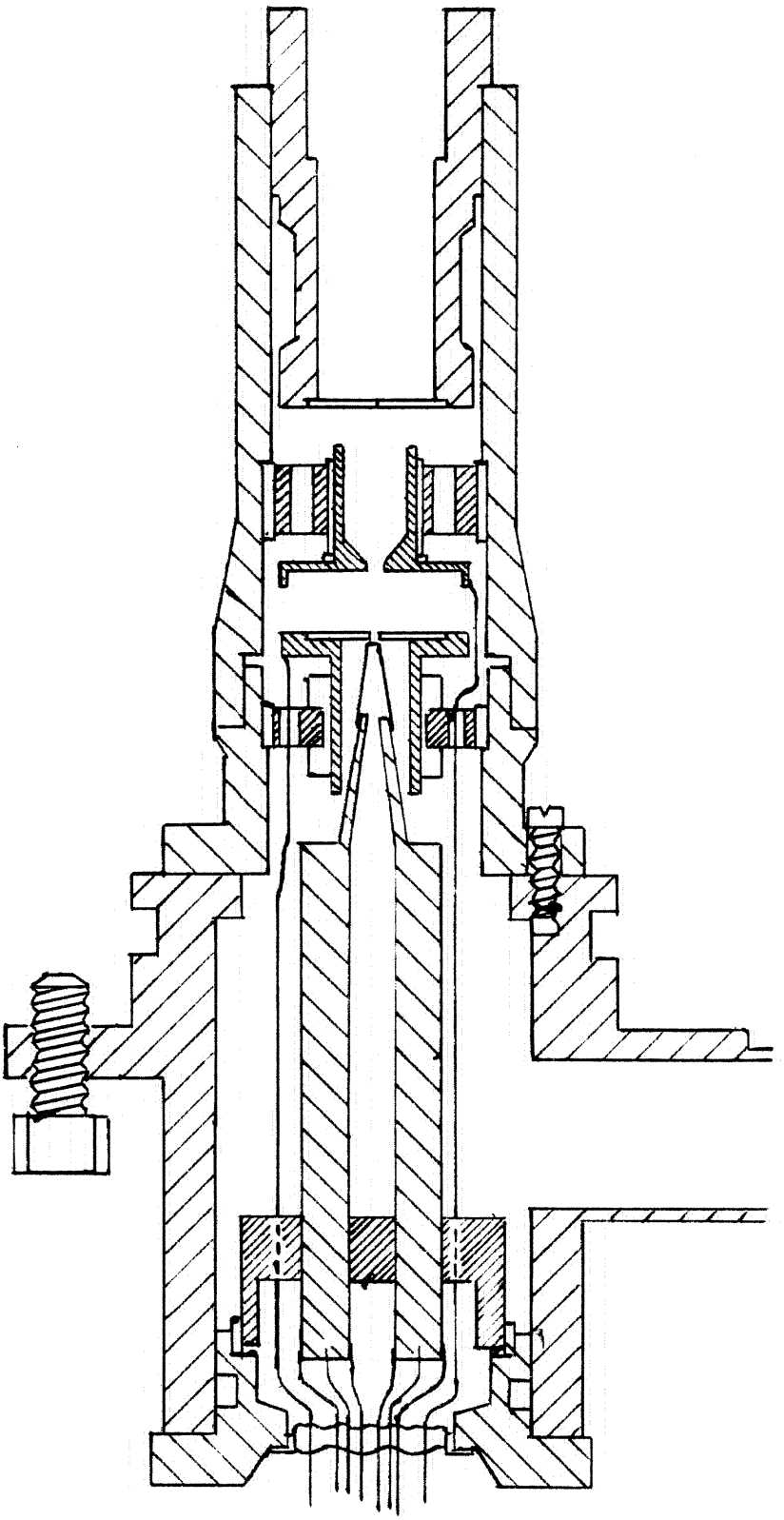

FIG.2 ELECTRON GUN

the vacuum header of the 100 liter/sec. oil diffusion pump. The vacuum header is sealed by an "O" ring to the flange at the end of the 4 foot aluminum tube, and with three bolts the vacuum header may be tilted about this "O" ring seal so that the electron gun may be aimed mechanically. A Kovar-glass seal containing the wires that present the potentials to the gun electrodes is soldered into a brass plug that seals by an "O" ring into the rear opening of the vacuum header. The tungsten electron gun filament is spot-welded to the two stainless steel tubes, 1/4" in diameter. These tubes are supported from the brass plug by a fired talc insulator and by the three wires from the glass seal that are spot-welded to each tube.

The gun electrodes are mounted in a cylindrical aluminum holder which is bolted to the front opening of the vacuum header in such a manner that the aluminum holder's axis may be aligned with the filament. All electrodes are mounted on precision machined cylindrical surfaces. The insulators are fired talc bushings that are banded interiorly and exteriorly with aluminum and then precision machined. The geometry insures that the electrodes are normal to the gun axis and centered with a high degree of accuracy. The aluminum holder is covered with a tight copper sheath that seals off the pumping holes in the holder so that the gun is separately pumped.

The electrode structure is quite simple yet it satisfies the several stringent requirements of the experiment. The electron beam must leave the gun at its full accelerating voltage, and the

fields at the filament must be independent of the total accelerating voltage. The final anode containing the .002" collimating pinhole is, therefore, grounded, and the entire accelerating voltage is placed on the filament. The potential of the grid directly in front of the filament and the first anode with respect to the filament is maintained constant. The geometry is such that the field penetration of the variable accelerating voltage is negligible. The usual potentials of the first anode and the grid with respect to the filament are respectively 300 volts positive and 1.5 volts negative. The negative grid voltage reduces grid current and minimizes the variation in emissivity of crystals in the tungsten filament. Since neither electrode draws current, both are battery supplied.

The focusing effect of the accelerating fields is small so that the beam is principally governed by the geometrical arrangement. The .020" pinhole in the molybdenum grid and the .002" pinhole in the final anode define the beam. Therefore, the solid angle subtended by the beam as it passes through the .002" collimating pinhole is rather insensitive to voltage. The diameter of the beam as it falls upon the phosphor screen at the center of the apparatus varies from .8" to .5" as the accelerating voltage varies from 2100 volts to 900 volts, as compared to the diameter of .8" predicted by rectilinear optics. The accurate alignment of the electrodes secures the beam direction as independent of voltage.

The filament is a directly heated thoriated tungsten wire shaped like a hairpin. The wire has a .013" diameter, but at the bend it has been hammered to a width of .022" and then ground flat. This flat surface is the emitting surface, and lies within a

few mils of the grid when hot. The grid is made of molybdenum and the grid holder of stainless steel to withstand the temperature rise. The filament must transmit several hundred microamperes through the .020" hole in the grid in order that the current detector at the opposite end of the vacuum tube receive the $2.5\ 10^{-12}$ amperes necessary for an accurate measurement. To accomplish this the filament must dissipate about 20 watts at a current somewhat greater than 8 amperes. Thus the potential drop across the filament is over 2 volts. However the effective surface contributing to the beam is about .020" in diameter with a potential drop of .04 volts which is small compared to the spread in thermal energy. The filament temperature is estimated to be $2000^{o}K$ so that kT=.17 volts. Even if only one velocity component contributes, the mean energy spread is .09 volts. The actual energy spread is probably several tenths of a volt. This voltage spread does not introduce systematic error, but it would improve resolution if it were smaller. Unfortunately it has been found that the lifetime of an oxide coated emitter in our oil pumped system is too short for its use to be practicable.

Any surface exposed to an electron beam in an oil pumped system has an insulating layer deposited. The .002" pinhole collimates the beam, and an insulating layer is formed in the vicinity. This layer at first broadens the beam leaving the pinhole, then reduces in a marked manner the beam stability, and finally will prevent the beam from passing through the pinhole. This effect is the principal obstacle to the collection of accurate data. No method of eliminating this difficulty has been discovered, and after too thick

a layer has developed this surface must be cleaned mechanically. By improved evacuation and the systematic cleaning of surfaces to minimize oil creepage the operating time before an unstable layer collects has possibly been doubled. The grid collects a small current and forms a deposit over a long period of time. This deposit must be cleaned periodically but involves no loss of time. The .004" pinhole beyond the cavity requires months for a deposit to be formed. Only essential surfaces are exposed to the beam.

Formation of positive ions by the electron beam raises difficulties when the vacuum is poor. To prevent the accumulation of these ions, all regions of the gun have accelerating fields to sweep ions out. It has become standard procedure to drive out occluded gases in the gun by running an AC discharge between the electrodes and ground while pumping the system down.

Dry cells furnish the grid and first anode voltages by wires passing through the Kovar glass seal. The voltage variation due to ambient temperature changes is not significant. The total accelerating voltage is applied to the center tap of a resistor across the electron gun filament. This voltage is furnished by a regulated power supply, Fig. 3, which was designed by W. T. Ogier and was described in his thesis. The output ripple is about 10 ppm at all voltages. The voltage is adjusted by using two switches that have 400 volt and 50 volt intervals respectively, and by using a Helipot with a 100 volt range that may be adjusted to an accuracy of better than .02 volts. The supply is not thermally regulated and is subject to slow drifts, but error due to this cause may be avoided by frequent measurements.

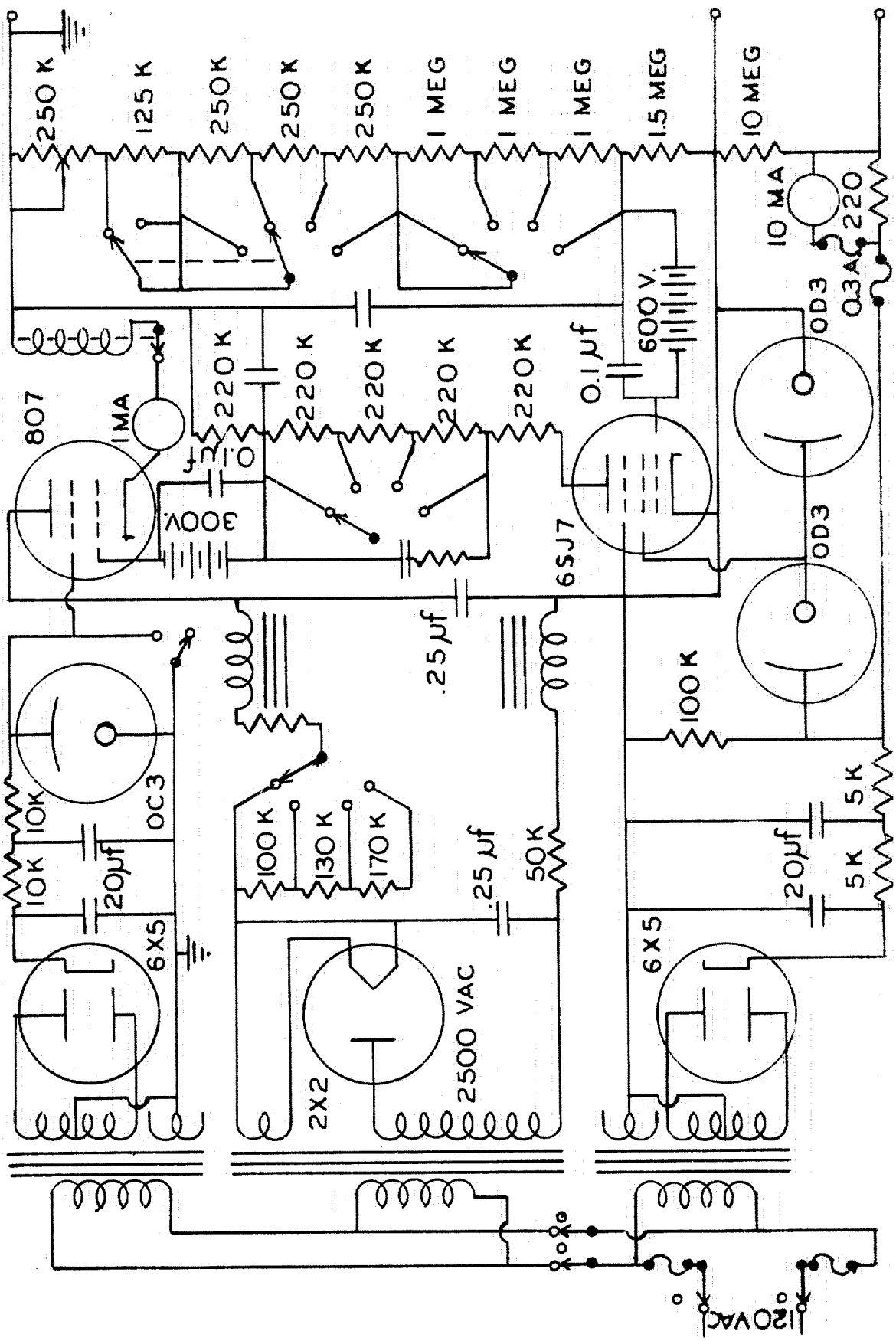

FIG 3. ACCELERATING VOLTAGE SUPPLY

The method by which this accelerating voltage is presented to the filament requires that the filament current be maintained constant. Beam stability requires that the filament current be constant with greater severity. The large current drawn from a storage battery produces too rapid a drift. The drift is reduced by the three storage battery circuit in Fig. 4a. The resistance of the rheostat, R, may be adjusted until the battery E_1 carries little load, and the remaining two batteries supply essentially the entire current. The output voltage, E, is

$$E = E_1 (1 - r/r+R) + (r/r+R)(E_2+E_3-IR)$$

The output drift is then improved by the factor $r/R < .008$. In practice it is observed that the output voltage decreases by 1% while the current carrying batteries decrease by 50%.

The remaining drift due to batteries, temperature effects in resistors, and rheostat contacts was controlled by an electronic regulating circuit, Fig. 4b. This circuit delivers 200 ma. in opposition to the filament current drawn from the battery supply. A fraction of the current supplied to the electron gun filament is passed through the filament of the diode, type 2AS-15, manufactured by Sorenson and Co., Inc. The filament of this tube is a straight thoriated tungsten wire lying along the axis of the plate, a right circular cylinder operated at 60 volts positive to the filament. The plate current then follows a temperature-limited tungsten emission curve, and for this reason the sensitivity of the diode is sufficient to regulate the electron gun filament current. The input signal to the regulator is the potential drop across the

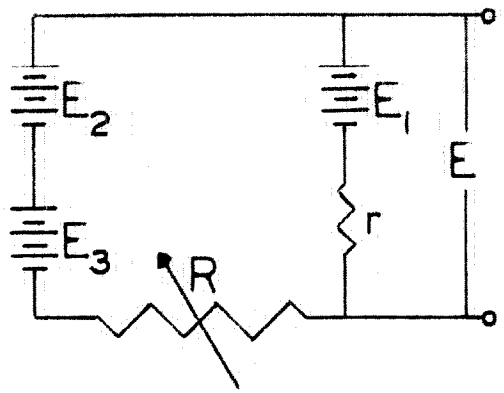

FIG. 4a. BATTERY DRIFT COMPENSATOR

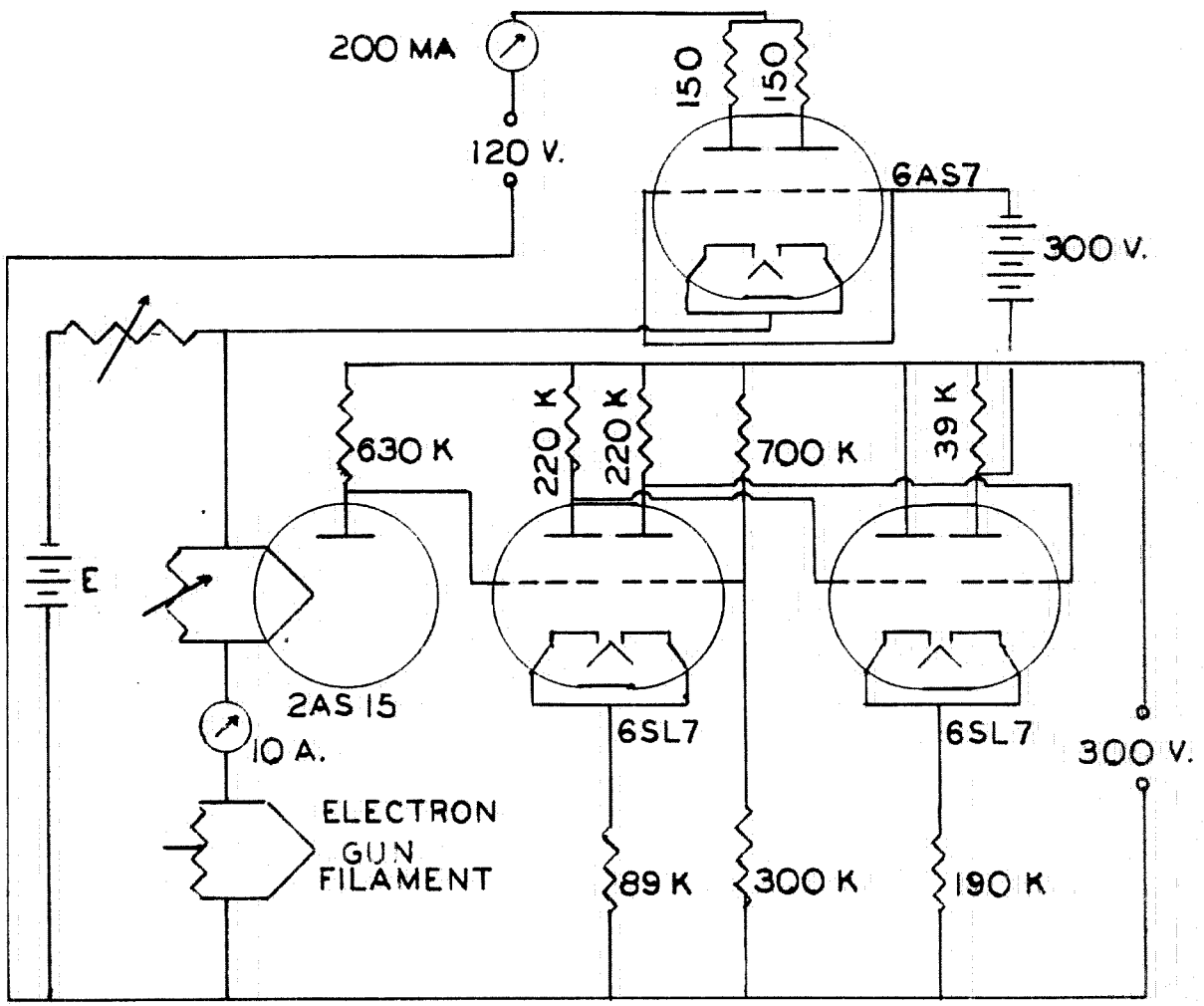

FIG. 4b. FILAMENT REGULATOR

630 K resistor due to the plate current of the 2 AS-15. This signal is amplified in two stages and drives the grid of the 6AS7 which furnishes the regulating current. The circuit elements are such that regulation occurs when the 6AS7 is delivering between 40 ma. and 200 ma. The steady battery drift will of course be followed by the regulating current. To maintain regulation the rheostat R_o must be adjusted so that the circuit regulates. This insures that the filament current is maintained constant to the necessary precision.

2.4 Voltage Measurement

The experiment requires that the accelerating voltage of the electron beam be measured with precision easily and quickly. The voltage is applied across a precision, high impedance voltage divider with a voltage division ratio of 1/1025. Since the accelerating voltage may vary from 700 to 2200 volts, the reduced voltage lies between .68 and 2.1 volts. A known voltage is opposed to the reduced voltage and the difference is measured by a precision low resistance potentiometer.

The accuracy attained by this measurement is limited by the uncertainty in the voltages of the standard cells which are used as comparisons. These are three Saturated Weston standard cells, which are maintained in a box thermally regulated within .002°C so that the standard cell voltage is constant. Two of these cells have a known history and are quite stable, while the remaining cell has an unknown history and undergoes appreciable drifts. The voltage of these three cells is determined by comparison with a bank of six saturated Weston cells that have been calibrated at the U. S. Bureau of Standards. The voltage of this bank of cells is

known to 10 ppm.

The bucking voltage, i. e. the voltage used in opposition to the reduced voltage, is obtained by dividing the output of a storage cell across two stable resistors. This bucking voltage is determined by comparing it with a standard cell. Occasionally, when the storage cell is being charged, a standard cell is used as the bucking voltage. This is avoided when possible since the storage cell cannot be hurt by a failure of the high voltage.

An O. Wolff Potentiometer (Serial No. 7521) and Auxiliary Box (Serial No. 7532) were used to measure voltage differences. This instrument has four ranges with maximum readings of 1.1, .11, 011, and .0011 volts respectively. The potentiometer is operated on its upper range since the measured voltages extend from -0.4 to 1.1 volts. A current of 0.1 amperes 10 volts drawn from storage cells supplies the working voltage of the potentiometer. A Leeds and Northrup Type E galvanometer with a sensitivity of .0004 μa/mm is used in conjunction with the potentiometer. The potentiometer may be read to 10 μv when measuring the reduced voltage and to 1 μv when comparing standard cells.

The potentiometer has been calibrated at the U. S. Bureau of Standards. The calibration on the upper scale is good to 100 ppm or 10 μv, whichever is greater. The accuracy that could be assigned to the potentiometer readings was, therefore, investigated rather carefully. Suppose that the reduced voltage to be measured is 2.1 volts. This may be opposed by one or two standard cells, leaving a voltage difference to be measured of about 1.1 and 0.1

volts respectively. The guaranteed accuracy of the potentiometer calibration in the two cases is 110 μv and 10 μv. Since the standard cell voltage is known, the larger reading may be calibrated to within 20 μv. This calibration seemed to be reliable, and checks were made with reasonable frequency. For this reason the full scale reading of the potentiometer was assigned an accuracy of 40 μv.

A switching circuit was provided so that all standard cells could be intercompared, and so that various bucking voltages could be opposed to the reduced voltage. Since all leads, terminals, and switches are copper, spurious thermal E.M.F.'s are believed completely negligible compared to desired accuracy of 10 μv. No measurable voltages have been observed to arise in the switch contacts. The leakage resistance between any two elements in the circuit is greater than 10^9 ohms so that no leakage error is introduced.

The voltage divider used in this experiment was constructed by Mr. J. N. Harris for use in a precision measurement of (h/e) at this laboratory[12], and was kindly loaned to this project by Dr. J. W. DuMond. The theory, construction, and operation of this remarkable instrument has been fully discussed by Mr. Harris[13]. A short discourse on the instrument and its use will be included here. Suppose that the "low" end of the divider consists of a resistor r, and that the "high" end of the divider consists of N resistors of mean resistance R and proportional deviation m_i:

$$R_i = R(1 + m_i) \qquad i = 1, 2, \ldots N$$

Let R_s and R_p be the resistance of the "high" end taken in series and in parallel. If $|m_i| < 10^{-3}$, then within 1 ppm

$$R_s/R_p = N^2 \left\{ 1 + 1/N \sum_{i=1}^{N} m_i^2 \right\}$$

The voltage dividing ratio is

$$R_s + r/r = N^2 R_p/r \left\{ 1 + 1/N \sum_{i=1}^{N} m_i^2 \right\} + 1$$

An absolute calibration of a resistor or a comparison between two unlike resistors is difficult to perform with precision. However, a comparison of nearly equal resistors by the bridge interchange method will yield great accuracy with comparative ease. Therefore, r is constructed approximately equal to R_p ($R_p \approx R/N$). Then $R_p/r = (1 + \epsilon)$ by measurement, and the voltage dividing ratio is

$$R_s + r/r = N^2 (1 + \epsilon) + 1$$

The ratio is determined by N so that a convenient value of R may be chosen. In the division of a large voltage R should be as large as leakage conditions permit so that the dissipated power is small.

The voltage divider contains one hundred 10,000 ohm resistors which have a maximum deviation from the mean of 0.50 ohms and a root mean square deviation of .16 ohms. These resistors are mounted in a large lucite box filled with high resistance oil. The oil is circulated by a motor-driven impeller, and a calrod heater maintains the oil at 33°C. There is space in the box to mount a dozen other resistors which form the "low" side of the divider.

In this experiment 32 groups of three 10,000 ohm resistors were used as the "high" end of the divider so that $R \approx 30,000$ ohms,

N = 32, $R_s \approx 960,000$ ohms, and $R_p \approx 937.5$ ohms. r was constructed to be 937.5 ohms from five 80 ohm resistors, three 133-1/3 ohm resistors, and two 100 ohm resistors taken in parallel to 15,000 ohms made up from three 10,000 ohm resistors. Then our voltage division ratio was

$$R_s + r/r = 1024\,(1 + \epsilon) + 1 = 1025 + 1024\,\epsilon$$

Using the Bridge Interchange Method ϵ was found to be $-1.5\ 10^{-5}$ and $-0.7\ 10^{-5}$ before and after all voltage measurements. Then the appropriate value for the voltage division during the experiment is 1024.99.

The power dissipated in the divider was always less than five watts, and it was found that no correction was necessary. No correction was necessary for leakage.

Mr. J. N. Harris built the thermally regulated box containing the standard cells and the equipment used in the resistance comparisons as well as the voltage divider. His excellent construction greatly facilitated this voltage measurement.

2.5 Electron Beam Detection Apparatus and Collimation

The electron beam detection apparatus is mounted on a moveable aluminum endplate. The beam is collected in a copper Faraday cup mounted to the endplate by a lucite rod. The electron secondary current is reduced to a negligible amount by gold-plating the Faraday cup, suitably shaping its interior, and by operating it 45 volts positive to ground. Before entering the cup the electron beam is collimated by a pinhole that was drilled in .005" copper sheet with a .008" pivot drill. This pinhole may be swung away to uncover the Faraday cup to the entire electron beam by rotating a

brass rod which passes through the endplate with an "O" ring seal. The pinhole and vicinity may be observed from outside the vacuum by means of a glass window and a mirror. If phosphor is placed about the pinhole the beam may be observed visually.

The beam current collected by the Faraday cup is presented to an electrometer circuit through a Kovar-glass seal waxed into the endplate. The detecting electrometer tube of this circuit, a sub-miniature CK 571-AX pentode, and its 10,000 megohm resistor are also mounted in the vacuum on wires from the glass seal, thus securing excellent shielding and leakage conditions. A copper box containing a hole to admit the beam surrounds the electrical elements.

The remainder of the electrometer circuit is mounted on the exterior of the endplate and is connected to the Kovar-glass seal by a short shielded cable. The electrometer circuit, Fig. 5, is discussed by Dr. W. T. Ogier in his thesis[9]. Two sub-miniature electrometer pentodes (CK 571-AX) are balanced against one another, and a filament rheostat compensates for filament drift. The input signal is the voltage developed across the 10,000 megohm grid resistor. The output signal is the unbalanced tube output, which is presented directly to a galvanometer through an Ayrton shunt. A Leeds and Northrup Type P mirror galvanometer with a sensitivity of .004 μa/mm is used, and the mirror spot is read on a 500 mm scale at a distance of 3 meters from the galvanometer. The electrometer is capable of registering a change of $5\ 10^{-16}$ amperes in beam current.

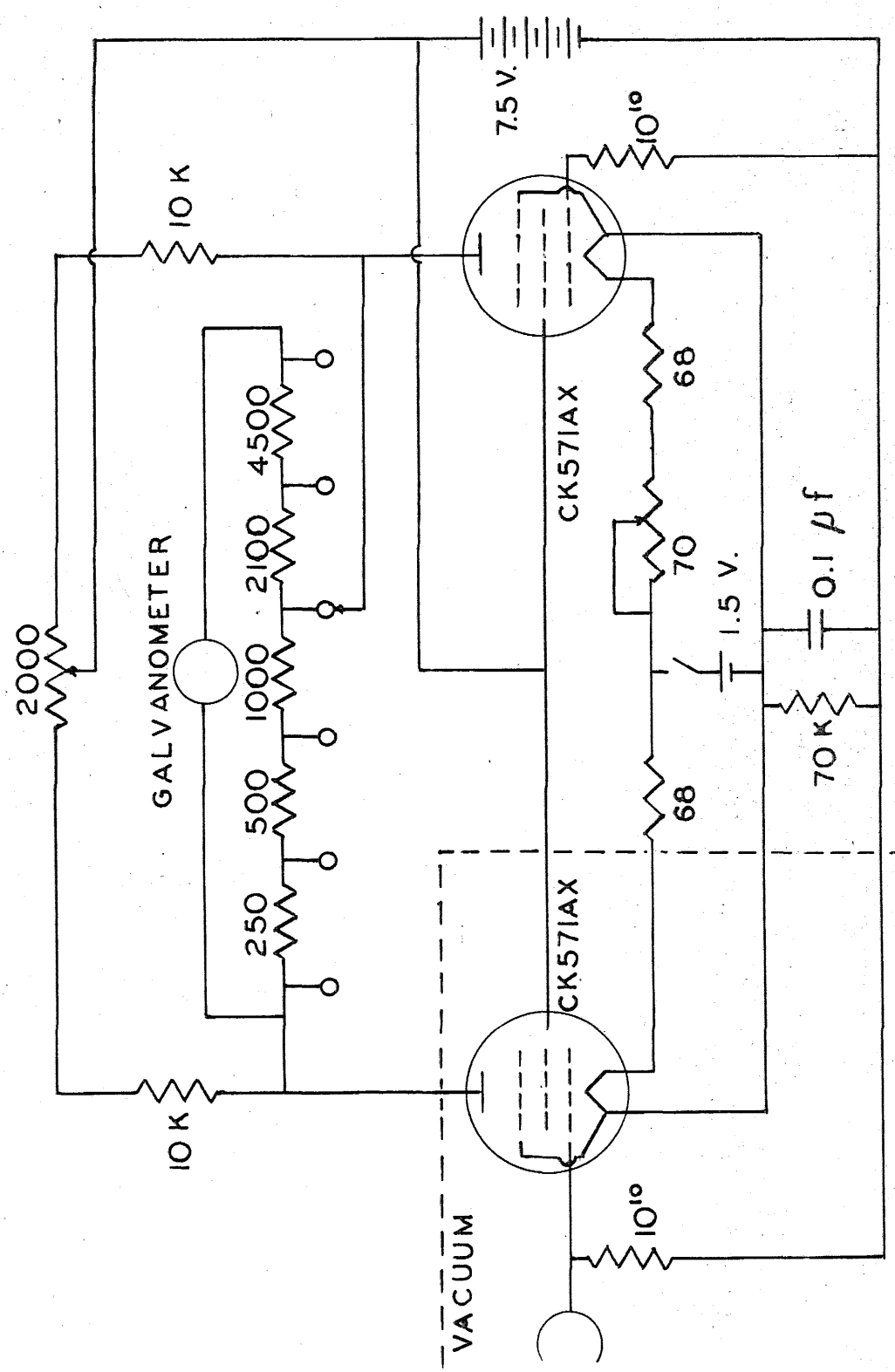

FIG. 5. ELECTROMETER CIRCUIT

A large plywood box covered with .005" copper foil surrounds the entire end of the vacuum envelope. This box, which is mounted on the wooden frame, insures adequate shielding for the electrometer which can be very sensitive to small fields.

The electron beam is collimated geometrically by the .002" pinhole in the electron gun and the .004" pinhole just beyond the resonant cavity. A geometric analysis established the diameter of the umbra at the collector pinhole as .006" and the diameter of the penumbra as .010". Optimum resolution is achieved for this distribution with the collector pinhole diameter lying between these values. Investigation shows that the electron beam actually has this general shape and dimensions, although the flat umbra is replaced by a gradually approached maximum at the center and the trailing edge of the penumbra is broadened to a somewhat greater diameter. Experimentally the diameter of the collector pinhole was chosen as .008", which agrees with theoretical expectations.

Optical alignment fails because of large diffraction patterns. Therefore, the mechanical construction must insure that the .004" pinhole is centered with the cavity. This pinhole is mounted centrally in the turning tube of the cavity endplate which should be centered with the cavity axis. This has been checked and found to be centered better than .002". During all measured peaks the electron gun exit pinhole has been within .030" of the center of the aluminum tube. The tilt of the resonant cavity with respect to the brass ring is less than one part in 1000. The angle between the electron beam and the cavity axis cannot be greater than 5 minutes, and it is probably much less.

Electric shielding is excellent. The charging of surfaces in the long drift spaces in the aluminum tubes is negligible. It has been found that electrostatic deflectors near high current beams rapidly charge up. For this reason the only electrostatic deflector is located beyond the cavity where the beam current is less than 10^{-10} amperes, and the maximum voltage applied to these plates is 1.5 volts. All additional alignment is accomplished mechanically.

The radius of curvature of a 2000 volt electron in the earth's magnetic field is about 35 centimeters. Leakage magnetic fields amounting to perhaps 1 gauss in intensity are caused by other instruments at this laboratory. Since it is desired to pass the electron beam about eight feet in an essentially geometric path, the magnetic shielding is extremely critical. The shielding described in 3.1 seems adequate for these requirements. When the magnetic field surrounding the instrument changes by an amount greater than the earth's field, the displacement of the electron beam at the collector pinhole is less than .020". During peak measurements magnetic field changes are at most a few per cent of a gauss, and usually much less.

Figure 6 is included to demonstrate the relationship of the electric circuits in the apparatus.

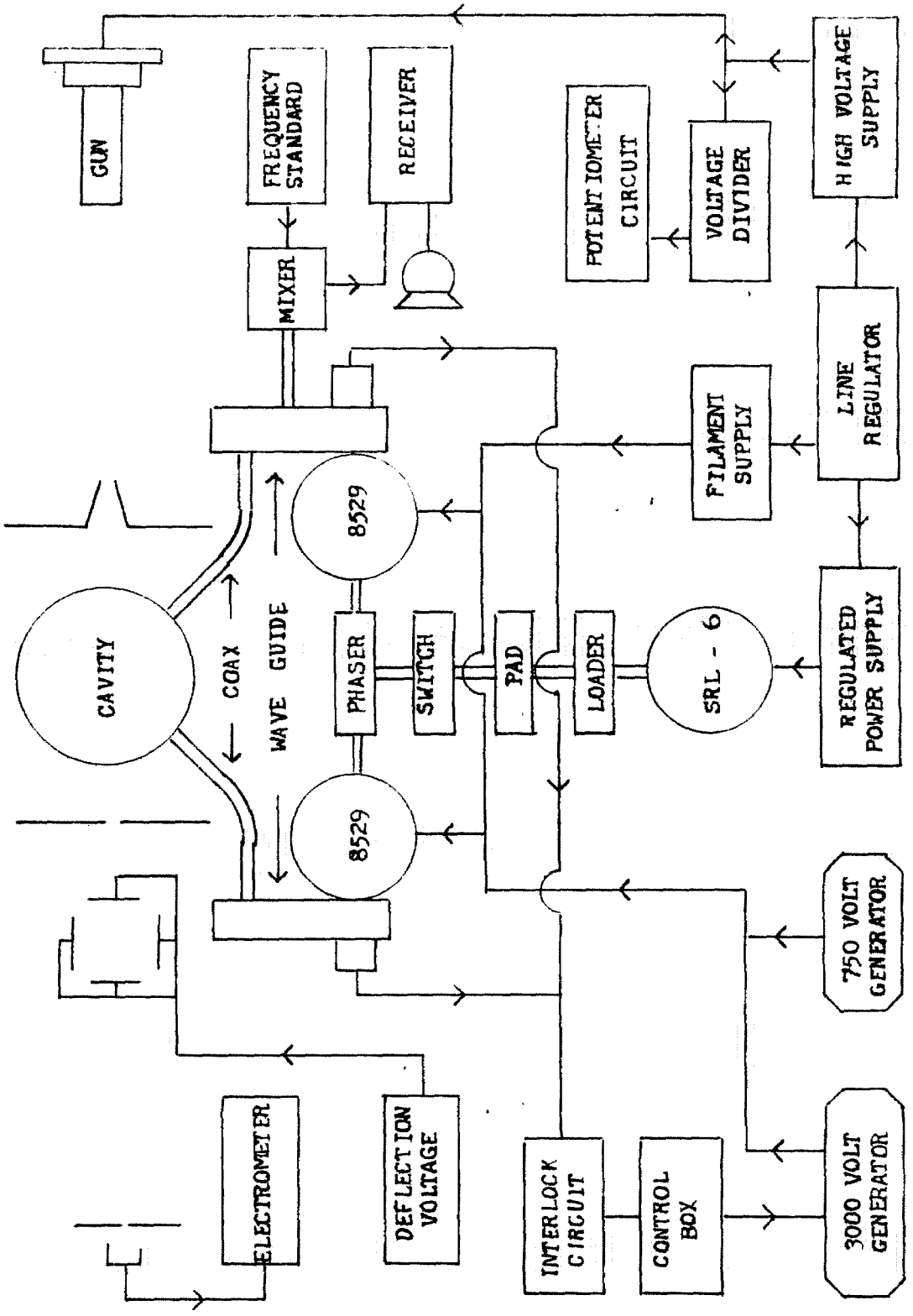

FIGURE 6. RELATIONSHIP OF ELECTRIC CIRCUITS.

III. THEORY OF THE EXPERIMENT

3.0 Radio Frequency Fields in Cavity without End Holes

The vector potential in cylindrical coordinates ρ, ϕ, z for a cavity bounded by the surfaces $\rho = b$, $Z = \pm \frac{1}{2}d$ and operated in the two orthogonal degenerate TM_{110} modes was obtained in Chapter 1.3.

$$\underset{\sim}{A}=\underset{\sim}{k}(2c/\omega)J_1(\omega\rho/c)\left\{B_1\sin\phi\cos\omega t-B_2\cos\phi\sin\omega t\right\} \qquad (1)$$

where $J_1(\omega b/c) = 0$, $(\omega b/c) = 3.8317$, $\omega = 2\pi f$.

The diameter of the cavity used in this experiment is 5.487 inches so that $f = 2.62\ 10^9\ (\text{sec.})^{-1}$. The cavity length is either $d = 1.1954$ inches or $d = 1.6295$ inches. Of all possible modes the TE_{210} and TE_{310} modes with frequencies $2.08\ 10^9$ sec.$^{-1}$ and $2.88\ 10^9$ sec.$^{-1}$ respectively are nearest in frequency to the TM_{110} mode. Only the TM_{110} mode will be excited when the cavity is driven at the correct frequency.

The flat ends of the cavity are chromium while the cylindrical surfaces are molybdenum. If μ_1, μ_2, and μ are the permeabilities of chromium, molybdenum, and the interior of the cavity respectively, and if δ_1 and δ_2 are the skin depths of chromium and molybdenum respectively, the cavity Q is[14]

$$Q=(\mu bd)(\mu_1\delta_1 b+\mu_2\delta_2 d)^{-1} \qquad (2)$$

This expression neglects the resistive loss between the cylindrical and flat surfaces which may be appreciable. The theoretical Q is about 8000. The average power loss is in MKS units.

$$\overline{P} = (\omega b)^2\left\{J_o(\omega b/c)\right\}^2 d(B_1^2+B_2^2)(2\mu fQ)^{-1} \qquad (3)$$

If B_1 and B_2 are measured in gauss, d in centimeters, and $\overline{P}$ in watts, equation (3) becomes

$$\overline{P} = 3200\ (d/Q)(B_1^2+B_2^2) \tag{4}$$

If $Q \sim 5000$, $d \sim 3$ cm., and $B_1 = B_2 = 5$ gauss, $\overline{P} \sim 100$ watts. The power that may be delivered to the cavity is the principal limit on the magnetic field strength. It will be shown that 5 gauss is not far from the optimum value for resolving the "resonant" voltage.

The magnetic and electric fields are obtained from the vector potential. Expanding these fields about the cavity axis and neglecting terms of third and higher degree in x and y, we obtain in gaussian units

$$B_x = B_1 \left\{1 - (\omega^2/8c^2)(x^2+3y^2)\right\} \cos\omega t + (\omega^2/4c^2)B_2 xy \sin\omega t \tag{5}$$

$$B_y = B_2 \left\{1 - (\omega^2/8c^2)(3x^2+y^2)\right\} \sin\omega t + (\omega^2/4c^2)B_1 xy \cos\omega t \tag{6}$$

$$E_z = (\omega/c)(B_1 y \sin\omega t + B_2 x \cos\omega t) \tag{7}$$

These fields, which are derived for a geometrically perfect cavity, are modified if the cavity walls are deformed. The effect of the holes in the flat endplates will be considered in the next section. The effect of slight bulges in the cylindrical surface is computed in Appendix I. If bulges centered about the points (x=b, y=z=0) and (x=0, y=b, z=0) on the cavity walls reduce the cavity volume by amounts δv_1 and δv_2 respectively, the fields near the axis are

$$B_x = B_1 \left\{1 - \frac{\omega^2(x^2+3y^2)}{8c^2} - \frac{\omega^2 \delta v_2}{bdc^2}\, y\right\} \cos\omega t + \frac{\omega^2 B_2 xy}{4c^2} \sin\omega t \tag{8}$$

$$B_x = B_2 \left\{ 1 - \frac{\omega^2(3x^2+y^2)}{8c^2} - \frac{\omega^2\,\delta v_2}{bdc^2}\,y \right\} \cos\omega t + \frac{\omega^2 B_2 xy}{4c^2} \sin\omega t \qquad (9)$$

$$E_z = (\omega B_2/c)\left\{x + (\delta v_1/\pi bd)\right\}\cos\omega t + (\omega B_1/c)\left\{y + (\delta v_2/\pi bd)\right\}\sin\omega t \qquad (10)$$

This approximation indicates the effect of the orifices in the cavity walls which furnish and detect R. F. power. The volume change due to these orifices is less than 0.14% of the cavity volume.

3.1 Radio Frequency Fields in Cavity with Circular End Holes

Two circular holes of radius a are centered in the plane end surfaces of the cavity. The cavity walls then correspond to the cylindrical surfaces $\rho = a$, $|z| \geq \frac{1}{2}d$; $\rho = b$, $-\frac{1}{2}d \leq z \leq \frac{1}{2}d$; and the plane surfaces $z = \pm \frac{1}{2}d$, $a \leq \rho \leq b$. The cavity fields for a single TM_{110} mode may be written in expanded form in terms of two scalar functions, W_1 and W_2.

$$\underset{\sim}{A} = \left\{\nabla \times (\underset{\sim}{k} W_1 + \underset{\sim}{k} \times \nabla W_2)\right\} \cos\omega t$$

$$\underset{\sim}{B} = -\left\{\nabla \times (\underset{\sim}{k}\omega^2 c^{-2} W_2 + \underset{\sim}{k} \times \nabla W_1)\right\} \cos\omega t$$

where

$$W_1 = \sum_{n=1} C_n \exp\left(\sqrt{k_n^2 a^{-2} - \omega^2 c^{-2}}\; z\right) J_1(k_n\rho/a)\cos\phi$$

$$W_2 = \sum_{n=1} D_n \exp\left(\sqrt{l_n^2 a^{-2} - \omega^2 c^{-2}}\; z\right) J_1(l_n\rho/a)\sin\phi \qquad -\infty < z \leq -\tfrac{1}{2}d$$

$$W_1 = \sum_{n=1} N_n \sinh\left(\sqrt{k_n^2 b^{-2} - \omega^2 c^{-2}}\; z\right) J_1(k_n\rho/b)\cos\phi$$

$$W_2 = \sum_{n=1} M_n \cosh\left(\sqrt{l_n^2 b^{-2} - \omega^2 c^{-2}}\; z\right) J_1(l_n\rho/b)\sin\phi \qquad -\tfrac{1}{2}d \leq z \leq \tfrac{1}{2}d$$

where k_n and l_n are defined by $J_1'(k_n) = 0$; $J_1(l_n) = 0$. These fields

satisfy both Maxwell's equations and the boundary conditions on the cylindrical surfaces. C_n, D_n, M_n, and N_n are coefficients which would be determined by satisfying the boundary conditions in the plane $z = -\frac{1}{2}d$. The evaluation of these constants is not feasible because of the extreme difficulty of solving the infinite set of equations. The general form of the solutions may be deduced, however.

By allowing $\rho = 0$ it may be shown that all field components vanish on the cavity axis except B_x and E_y. The expansions containing undetermined coefficients do not yield significant information, and it is sufficient to represent the axial fields by

$$B_x(\rho = 0) = BF(z)$$
$$E_y(\rho = 0) = -(\omega B/c)G(z)$$

where $F(z) = F(-z)$ and $G(z) = -G(-z)$. The circular entrance holes do not affect the simple ϕ-dependence of the TM_{110} mode. Application of Maxwell's Equations with this in mind secures the fields near the cavity axis in terms of F(z) and G(z):

$$B_x = BF(z)\cos\omega t \qquad E_x = 0$$

$$B_y = 0 \qquad E_y = -(\omega B/c)G(z)\sin\omega t \qquad (1)$$

$$B_z = Bx\left\{F'(z)+(\omega/c)^2 G(z)\right\}\cos\omega t \qquad E_z = (\omega B/c)y\left\{F(z)-G'(z)\right\}\sin\omega t$$

where quadratic and higher order terms in $(\omega x/c)$ and $(\omega y/c)$ are neglected.

Approximations for F(z) and G(z) must be known in order to obtain numerical results. A difficult calculation by Dr. W. R. Smythe has yielded an excellent approximation for F(z)[15]. This

approximation is the static magnetic solution for a uniform magnetic field parallel to the plane face of a nonpermeable substance containing a circular hole of radius a. Dr. Smythe has shown that the function F(z) obtained in his paper may be put in the form

$$\left.\begin{aligned} F(z) = {} & 0.8285\exp\{1.8412u(z)\} - 0.234\exp\{5.1u(z)\} \\ & + 0.340u(z)\exp\{6.2u(z)\} - 0.0036\exp\{17.6u(z)\} \end{aligned}\right\} -\infty < u \leq 0.1 \qquad (2)$$

$$\left.\begin{aligned} F(z) = {} & 1 - 0.046\exp\{-.75u(z)\} + 0.014\exp\{-u(z)\} \\ & - 0.3344\exp\{-2u(z)\} - 0.341\exp\{-4u(z)\} \\ & + 0.4832\exp\{-6u(z)\} - 0.1878\exp\{-8u(z)\} \end{aligned}\right\} 0.1 \leq u \leq \left(\frac{d}{2a}\right) \qquad (3)$$

where $u(z) = (z + \frac{1}{2}d)a^{-1}$. Since F(z) is a symmetric function we have an approximation that is valid over the range $-\infty < z < \infty$.

An accurate expression for G(z) is not known by the author, but a rough approximation may be obtained. Clearly $G(-\infty) = 0$, and, since G(z) is an odd function of z, $G(0) = 0$. Dr. Smythe's solution demonstrates the localization of the perturbation fields about the entrance hole so that near the center of the cavity

$$-c^{-1}(\partial B_x/\partial t) = (\partial E_z/\partial y)$$

as in the unperturbed mode. Comparison with the expression for E_z in equation (1) above shows that $G'(z) \longrightarrow 0$ as $z \longrightarrow 0$.

The most reasonable simple representation of G(z) is

$$G(z) = aF'(z) \qquad (4)$$

F'(z) vanishes in regions remote from the entrance hole both inside

and outside the cavity and is an odd function of z. It attains its greatest magnitude near the plane of the flat cavity walls, which is reasonable because the transverse electric field arises from the capacitive transmission of the cavity wall current across the entrance hole. At worst no more plausible justification can be given for a more complicated assumption.

To evaluate the constant a the magnetic field solution of Dr. Smythe's will be considered. Since this is a static solution the curl of the magnetic field vanishes, and the corresponding electric field is obtained by integrating the equation

$$\nabla \times \underset{\sim}{E} = -c^{-1}(\partial \underset{\sim}{B}/\partial t) \ .$$

This obtains the result

$$E_z = 0; \qquad E_y(\rho=0, z) = (1/c)\int_{-\infty}^{z} (\partial B_x/\partial t)\Big|_{\rho=0} dz \tag{5}$$

The expression for E_y is obviously erroneous in the interior of the cavity, but it is probably satisfactory at the cavity wall, $z = -\frac{1}{2}d$.

From equations (1) and (5)

$$G(-\tfrac{1}{2}d) = \int_{-\infty}^{-\frac{d}{2}} F(z)\, dz \tag{6}$$

Combining (4) and (6)

$$a = \left\{F'(-\tfrac{1}{2}d)\right\}^{-1} \int_{-\infty}^{-\frac{d}{2}} F(z)dz = 0.649a^2 \tag{7}$$

Combining these results with equation (1) we obtain an approximate representation of the cavity fields.

$$
\begin{aligned}
B_x &= BF(z)\cos\omega t \\
B_y &= 0 \\
B_z &= Bx\ \left\{1 + 0.649(\omega a/c)^2\right\} F'(z)\cos\omega t \\
E_x &= 0 \\
E_y &= -0.649(\omega a^2 B/c)F'(z)\sin\omega t \\
E_z &= (\omega B/c)y\ \left\{F(z) - 0.649a^2F''(z)\right\}\ \sin\omega t
\end{aligned}
\tag{8}
$$

A very important property of the cavity fields is their localization about the entrance holes. For all cavity lengths d used in this experiment $F(0) = 1$, i.e. the fields of the two circular entrance holes do not interfere. Investigation of equations (2) and (3) shows that $F(z)$ depends only upon the distance from the entrance hole, i.e. z enters the expression only in the form $(z + \frac{1}{2}d)$. Then if $F_1(z)$ and $F_2(z)$ are the axial magnetic field distributions for two cavities with lengths d_1 and d_2 where $d_2 > d_1$:

$$
\begin{aligned}
&F_1(w-\tfrac{1}{2}d_1) = F_2(w-\tfrac{1}{2}d_2) \qquad -\infty < w \leqslant \tfrac{1}{2}d_1 \\
&F_2(z) = 1 \qquad\qquad -\tfrac{1}{2}(d_2-d_1) \leqslant z \leqslant 0
\end{aligned}
\tag{9}
$$

The same holds accurately for $G(z)$ with no approximation so that

$$
\begin{aligned}
&G_1(w-\tfrac{1}{2}d_1) = G_2(w-\tfrac{1}{2}d_2) \qquad -\infty < w \leqslant \tfrac{1}{2}d_1 \\
&G_2(z) = 0 \qquad\qquad -\tfrac{1}{2}(d_2-d_1) \leqslant z \leqslant 0
\end{aligned}
\tag{10}
$$

3.2 First Order Solutions of Equations of Motion

The equations of motion of an electron in an electromagnetic field in gaussian units are

$$\frac{d}{dt}(m\underset{\sim}{v}) = -e\underset{\sim}{E} - (e/c)\underset{\sim}{v}\times\underset{\sim}{B} \tag{1}$$

where e is the magnitude of the electronic charge. The procedure of solution of these equations will be by direct integration under simplifying assumptions, followed by iteration to obtain more accurate solutions.

The fields for a single mode in the resonant cavity were derived in the last section. Extending these results to include two modes, and neglecting quadratic and higher order terms in $(\omega x/c)$ and $(\omega y/c)$, the fields are

$$B_x = B_1 F(z)\cos\omega t \tag{2}$$

$$B_y = B_2 F(z)\sin\omega t \tag{3}$$

$$B_z = \left\{F'(z) + (\omega/c)^2 G(z)\right\}\left\{B_1 x\cos\omega t + B_2 y\sin\omega t\right\} \tag{4}$$

$$E_x = -(\omega B_2/c)G(z)\cos\omega t \tag{5}$$

$$E_y = -(\omega B_1/c)G(z)\sin\omega t \tag{6}$$

$$E_z = (\omega/c)\left\{F(z) - G'(z)\right\}\left\{B_1 y\sin\omega t + B_2 x\cos\omega t\right\} \tag{7}$$

For the first order solution it will be assumed that the electrons remain so near the cavity axis that all terms depending on x and y may be neglected. In addition the z-component of velocity, $v_z = v$, and the relativistic electron mass, $m = m_o\left\{1-(v/c)^2\right\}^{-\frac{1}{2}}$, will be assumed constant. Then

$$z = v\,(t-T)$$

and direct integration of the transverse equations of motion obtains the change in the transverse velocity due to the cavity fields. $F(z)$ and $G(z)$ are negligible when $|z| \geq d$, and the lower limit of the integration may be taken as $(-d)$. The dependence upon the phase of entry into the cavity is clarified if a rotating set of coordinates ξ, η, are defined:

$$\dot{\xi}(z) = v \int_{-d}^{z} \left\{F(z)\cos(\omega z/v) - (\omega/v)G(z)\sin(\omega z/v)\right\} d(\omega z/v) \tag{8}$$

$$\eta(z) = v \int_{-d}^{z} \left\{F(z)\sin(\omega z/v) + (\omega/v)G(z)\cos(\omega z/v)\right\} d(\omega z/v) \tag{9}$$

Then the transverse velocities by direct integration are

$$v_x(z) - v_x(-d) = (b_2/\omega)\left\{\dot{\eta}(z)\cos\omega T + \dot{\xi}(z)\sin\omega T\right\} \tag{10}$$

$$v_y(z) - v_y(-d) = (b_1/\omega)\left\{\dot{\eta}(z)\sin\omega T - \dot{\xi}(z)\cos\omega T\right\} \tag{11}$$

where $b_{1,2} = (e/mc)_{esu} B_{1,2} = (eB_{1,2}/m)_{emu}$. The net change in the transverse velocities due to the cavity is obtained by setting $z \geq d$ in equations (10) and (11). Since $F(z)$ and $G(z)$ are even and odd functions in z respectively,

$$\dot{\xi}(d) = 2v \int_{-d}^{o} \left\{F(z)\cos(\omega z/v) - (\omega/v)G(z)\sin(\omega z/v)\right\} d(\omega z/v) \tag{12}$$

$$\dot{\eta}(d) = 0. \tag{13}$$

Then the change in transverse velocity is

$$v_x(d)-v_x(-d) = (b_2/\omega)\,\dot{\xi}(d)\,\sin\omega T \tag{14}$$

$$v_y(d)-v_y(-d) = -(b_1/\omega)\,\dot{\xi}(d)\,\cos\omega T \tag{15}$$

From (14) and (15) the angular deflection of the electron is

$$\theta = \left\{(b_1/\omega)^2\cos^2\omega T+(b_2/\omega)^2\sin^2\omega T\right\}^{\frac{1}{2}}\left|\dot{\xi}(d)/v\right| \tag{16}$$

This equation applies to a single electron which is at the center of the cavity when t = T. The electron beam contains electrons corresponding to all values of T, so that the beam is spread into a cone of elliptical cross section. The size but not the shape of this ellipse changes as the electron velocity varies. It will be shown in Section 3.4 that the current collected from a beam spread in this manner, when plotted against the accelerating voltage, forms a resonant peak with straight sides. The intersection of these sides occurs at the voltage where $\theta = 0$. Then the "resonant" velocity is obtained by solving the following equation:

$$\dot{\xi}(d) = \int_{-d}^{o}\left\{F(z)\cos(\omega z/v)-(\omega/v)G(z)\sin(\omega z/v)\right\}d(\omega z/v)=0 \tag{17}$$

In Appendix II an analysis of this equation and equations 3.1 (9) and (10) demonstrates that the solution has the form

$$(\omega/v)\left\{d + \Delta d(v)\right\} = 2n\pi \tag{18}$$

The "resonant" velocities, v_n, may be obtained, and thereby (e/m_o), if $\Delta d(v)$ is precisely known. Measurements performed for two different cavity lengths will determine $\Delta d(v)$ with sufficient precision,

if the functional form of $\Delta d(v)$ is known or if the variation of $\Delta d(v)$ with v is slight. Lack of exact knowledge of G(z) precludes learning the exact form of $\Delta d(v)$. The expected variation of $\Delta d(v)$ may be estimated by substituting the approximation for G(z) of equations 3.1 (4) and (7) into equation 3.2 (17):

$$\begin{aligned}\dot{\xi}(d) &= 2v\int_{-d}^{o}\left\{F(z)\cos(\omega z/v) - 0.649(\omega a^2/v)F'(z)\sin(\omega z/v)\right\}d(\omega z/v) = 0\\ &= 2v\left\{1+0.649(\omega a/v)^2\right\}\int_{-d}^{o}F(z)\cos(\omega z/v)\,d(\omega z/v) = 0 \qquad (19)\\ &= -(2v^2/\omega)\left\{1+0.649(\omega a/v)^2\right\}\int_{-d}^{o}F'(z)\sin(\omega z/v)\,d(\omega z/v) = 0\end{aligned}$$

If F'(z) is symmetrical about the point $z=-\frac{1}{2}(d+\Delta d)$ and vanishes at z = -d and z = 0, it may be seen from the last form of equation (19) that the solution of $\dot{\xi}(d) = 0$ will be

$$(\omega/2v)(d+\Delta d) = n\pi$$

Then the increment Δd is independent of voltage when the axial magnetic field derivative is symmetrical about some point. The magnetic field solution of Dr. Smythe differs but slightly from this condition, and by substituting his expression for F(z), equations 3.1(2) and (3), into equation (19) the following values of d(v) are obtained:

(v/c)	$\frac{1}{2}\Delta d(v)$	V	
0.05373	0.01871 cm.	739 volts	2a=0.0899 inches
0.06084	0.01892 cm.	948 volts	$f=2.6200\ 10^9$ (sec.)$^{-1}$
0.06717	0.01901 cm.	1157 volts	
0.07301	0.01904 cm.	1367 volts	
0.08251	0.01902 cm.	1748 volts	
0.08956	0.01897 cm.	2062 volts	
0.09126	0.01896 cm.	2141 volts	

In this experiment the accelerating voltage ranged between 730 volts and 2130 volts. The variation in $\{\Delta d(v)/d\}$ in the above table over this voltage range is 200 ppm. The table was derived for good and rough approximations of F(z) and G(z) respectively. It would appear reasonable to suppose that a more exact value of $\{\Delta d(v)/d\}$ would also vary by only a few parts in ten thousand over this voltage range.

Under the same assumptions for the cavity fields the deflection sensitivity is

$$(d\theta/dV) = 1.2\left\{(b_1/\omega)^2\cos^2\omega T+(b_2/\omega)^2\sin^2\omega T\right\}^{\frac{1}{2}}(n\pi/V) \qquad (20)$$

Although the leading coefficient in equation (20) is slightly dependent on n, the expression is correct to within 8% for all peaks. The slopes of the sides of the current peak are proportional to the time average of $(d\theta/dV)$ over all T. The term $(d^2\theta/dV^2)$ is so small that the difference in slopes of the upper and lower sides of a current peak is less than 1%. This does not shift the intersection of the sides although the peak is slightly "skewed".

Another effect that alters the shape of the current peak but does not displace the intersection of the sides is due to the displacement of the electrons while traversing the cavity. This displacement is obtained by direct integration of equations (10) and (11):

$$x(z)-x(-d)=(z+d)v_x(-d)/v+(b_2/\omega)\left\{\eta(z)\cos\omega T+\xi(z)\sin\omega T\right\} \qquad (21)$$

$$y(z)-y(-d)=(z+d)v_y(-d)/v+(b_1/\omega)\left\{\eta(z)\sin\omega T-\xi(z)\cos\omega T\right\} \qquad (22)$$

where

$$\xi(z)=(z/v)\dot{\xi}(z)-\int_{-d}^{z} z\left\{F(z)\cos(\omega z/v)-(\omega/v)G(z)\sin(\omega z/v)\right\}d(\omega z/v) \qquad (23)$$

$$\eta(z)=(z/v)\dot{\eta}(z)-\int_{-d}^{z} z\left\{F(z)\sin(\omega z/v)+(\omega/v)G(z)\cos(\omega z/v)\right\}d(\omega z/v) \qquad (24)$$

Substituting our approximations for F(z) and G(z) we find that near a resonance

$$\xi(d) = 0; \qquad \eta(d) = 1.2d \qquad (25)$$

The electron beam is collimated by circular pinhole, .004 inches in diameter, following the cavity. Then for any value of T a circle of .004 inches diameter is selected from the beam entering the cavity. It is sufficient for our purposes to consider the central electron of this circle as typical. The electrons that leave the cavity at $x(d) = y(d) = 0$ are selected from an ellipse with axes $2(b_1/\omega)\eta(d)$ and $2(b_2/\omega)\eta(d)$. The electron gun may be considered a point source so that spacial distribution at the entrance of the cavity may be attributed to geometric spread in velocities at the gun. In the simple case when the electron source lies on the cavity axis

$$v_x(-d) = (v/L)x(-d); \quad v_y(-d) = (v/L)y(-d) \qquad (26)$$

where L=50 inches and is the distance between the electron source and the cavity.

The electrons at resonance are undeflected so that they leave the collimating pinhole with their entering velocities and form a cone of elliptic cross section. Since the distance between

the cavity and collector is approximately equal to the distance between gun and cavity, the beam at the collector will form an ellipse with axes $2(b_1/\omega)\eta(d)$ and $2(b_2/\omega)\eta(d)$. Then the current collected at resonance will be less than that received with the R. F. off.

An analysis of equations (14), (15), (21), (22), and (25) shows that angular spread near resonance is

$$\theta = \left\{(v_x(d))^2 + (v_y(d))^2\right\}^{\frac{1}{2}} v^{-1}$$
$$= \left\{\dot{\xi}^2(d)/v^2 + \eta^2(d)/L^2\right\}^{\frac{1}{2}} \left\{(b_1/\omega)^2 - (b_1^2 - b_2^2)\omega^{-2}\sin^2(\omega T')\right\}^{\frac{1}{2}} \quad (27)$$

where the origin of T' is unimportant since the electrons in the beam correspond to all values of T'. $\eta(d)$ is constant over the voltage change of the current peak, while $\dot{\xi}(d)$ varies in a linear manner with voltage. It is clear then that the peak shape will be changed but that the intersection of the sides will correspond to $\dot{\xi}(d) = 0$. A more detailed calculation, where the electron source and exit pinhole are permitted to be off axis, reaches the same conclusions.

3.3 Discussion of More Exact Solutions for Electron Trajectories

In the preceding section the electron trajectories were obtained on the basis of a first order theory. The anticipated accuracy of this experiment would require a more precise knowledge of the trajectories. This may be accomplished by a single iteration, substituting the first order solutions of velocity and displacement into the equations of motion and obtaining more exact expressions.

The experimental results do not justify such precision, and the iteration process involves very complicated expressions which obscure, rather than illuminate, the physical behavior of the electrons. For this reason the iteration procedure will only be sketched and the order of magnitude of the results mentioned.

The measured quantity is the electron beam current as a function of voltage, and this depends upon the angular deflection of the beam from the center of the pinhole. This angular deflection is

$$\theta = \left\{\theta_o^2 + (\Delta v_x/v)^2 + (\Delta v_y/v)^2\right\}^{\frac{1}{2}} \tag{1}$$

where Δv_x and Δv_y are the changes in transverse velocity due to the cavity fields, and θ_o is an essentially constant term arising from the spread in transverse velocities of the beam entering the cavity. The change in transverse momenta are

$$\Delta(mv_x) = -e \int_{-d}^{d} \left\{E_x - (v_z/c)B_y + (v_y/c)B_z\right\} (v_z)^{-1} dz \tag{2}$$

$$\Delta(mv_y) = -e \int_{-d}^{d} \left\{E_y + (v_z/c)B_x - (v_x/c)B_z\right\} (v_z)^{-1} dz \tag{3}$$

where all terms in the integrands are expressed as functions of the electron's position, z. The first order solutions for x, y, v_x, and v_y are substituted into their proper places in the integrand. In the substitution for t it is no longer sufficient to treat v_z as constant, and its variation due to electric fields and kinetic reaction terms must be included:

$$v_z = v\left\{1 - \chi'(z)\right\}$$

$$v(t-T) = z + \chi(z)$$

$\chi(z)$ is determined by the substitution of the first order solutions into the equations

$$\Delta(mv_z) = -e\int_{-d}^{z}\left\{E_z+(v_x/c)B_y-(v_y/c)B_x\right\}'v^{-1}dz \tag{4}$$

$$\Delta m(z) = -(e/c^2)\int_{-d}^{z}\left\{E_x dx+E_y dy+E_z dz\right\} \tag{5}$$

Evaluation of equation (5) shows that m(d) is negligible so that $\Delta(mv_x) = m\Delta v_x$ and $\Delta(mv_y) = m\Delta v_y$ in equations (2) and (3). Substitution of these results into equation (1) yields an accurate value of the angular deflection, θ.

This expression for θ shows that for a perfectly aligned beam the intersection of the straight sides of the peak will differ from first order theory by several parts in ten thousand and that this shift is proportional to $(b_1/\omega)^2 \approx (b_2/\omega)^2$. The resonant voltage has the form

$$v = (f/n)\left\{d + \Delta d(v) + a(c)(b/\omega)^2\right\} \tag{6}$$

where $\Delta d(v)$ is independent of the magnetic field strength. The effect of any possible misalignment is to produce a term in equation (1) with the same form as θ_o so that no change in "resonant" velocity results.

The magnitudes of some of these quantities is of interest. The quadratic terms in x and y in the cavity fields cause variations of about 10 ppm, and the higher order terms are much smaller.

The linear terms are more important. The variation in v_z amounts to about one part in a thousand, since the electron loses as much as several volts to the z component of the electric field at one point in its traversal of the cavity. Nevertheless, the net energy change of the electron in crossing the cavity is negligible when near resonance. This is due to the fact that the electron is decelerated in the first and last quarter cycles that it remains in the cavity and is alternately accelerated and decelerated in the intervening half cycles. While the transverse electric fields may amount to 50 volts/cm., they are localized near the entrance holes. The energy change due to these fields at no point amounts to more than 0.1 volts, and this change is canceled over a complete traversal.

It should be noted that the "resonance" criterion has been applied to the z component of velocity. If the electron source deviates from the cavity axis by an angle, ϕ, the total velocity, v_t, corresponding to the measured voltage is related to the axial velocity, v_z, by

$$(v_t/v_z) = \cos\phi$$

and the fractional error introduced to (e/m_o) is $(1-\cos^2\phi)$. Care in the geometry of the instrument reduces this to 6 ppm or less.

3.4 Collection of Current

The electron beam is received in a Faraday cup after passing through a circular pinhole with a .008 inch diameter. The current received is a function of the distance between the centers of the pinhole and the beam, and attains a maximum when the centers coincide. The geometrical collimation of the beam produces a

density distribution with an umbra and penumbra, such that 55% to 70% of the total electron current is collected when the beam is centered.

Under normal operating conditions the beam is circularly symmetric, and the collected current depends only upon the magnitude of the beam displacement. The received current has been determined empirically as a function of mechanical displacement, and the result is plotted in Fig. 7. The most important characteristic of this curve is that it is linear over a considerable range of displacement.

The electrons leaving the exit pinhole of the cavity at one instant will have an angular deflection $\dot{\theta} = \theta(\omega T)$ depending periodically upon T, a time specifying the phase of the electrons' entry into the cavity. The displacement at the collector of this circular beam is

$$D(\omega T) = L\theta(\omega T) \tag{1}$$

where L is the distance between cavity and collector.

The instantaneous current received is independent of the displacement and depends upon its magnitude in the manner shown in Fig. 7. The intersection of the linear sides of this curve determines the "resonant" voltage so that only the linear section will be considered. The instantaneous current is

$$I(\omega T) = A - BD(\omega T) \tag{2}$$

where A and B are constants.

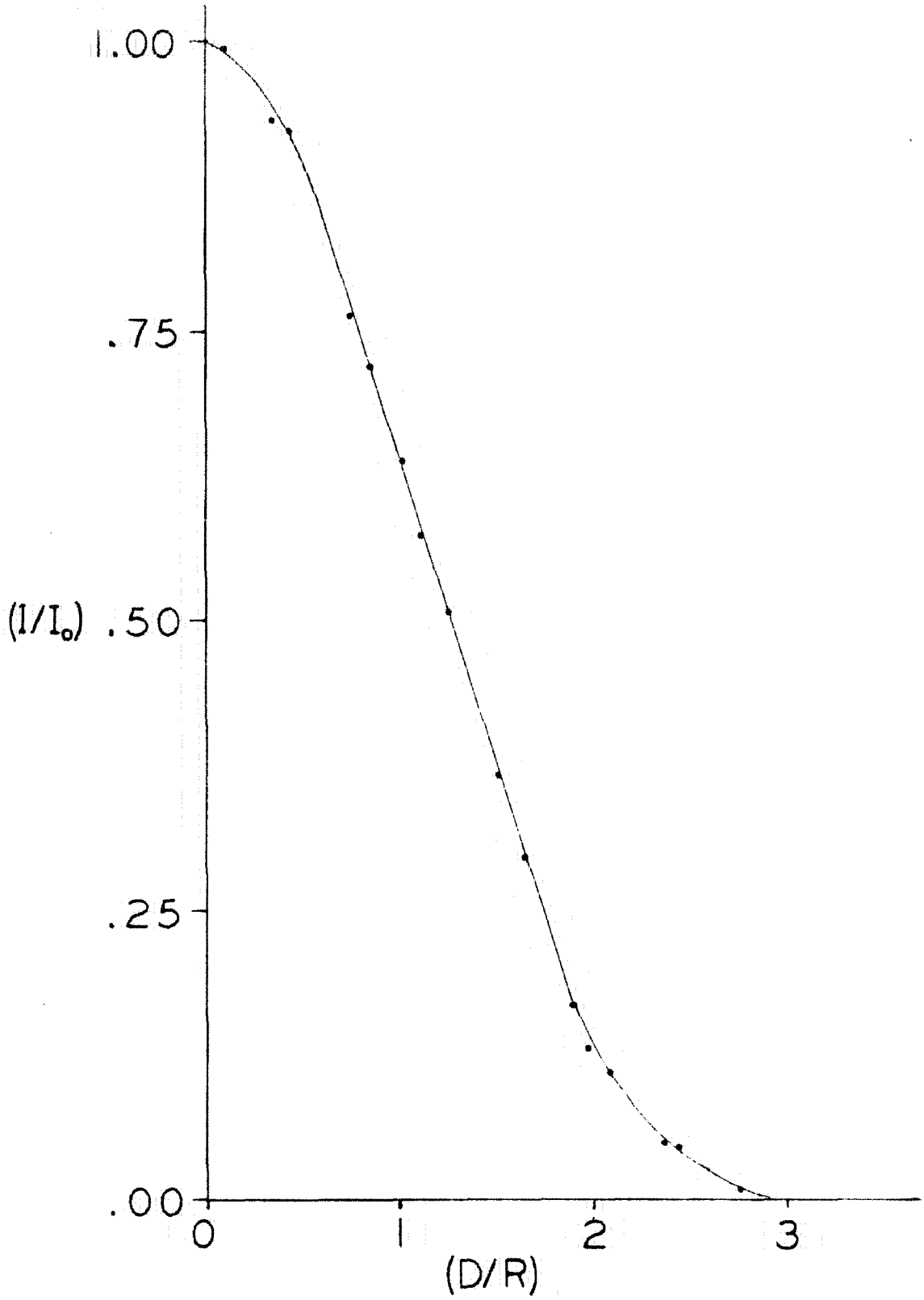

FIG. 7 CURRENT VERSUS BEAM DISPLACEMENT

The electrometer is too slow to follow the fluctuations of (ωT) which possess the cavity frequency of 2620 megacycles. The measured current is the time average of the instantaneous current, and is

$$\bar{I} = (1/2\pi)\int_0^{2\pi} I(\omega T)d(\omega T) = (1/2\pi)\int_0^{2\pi}\{A-B(\omega T)\}d(\omega T) = A-B\overline{D(\omega T)} \qquad (3)$$

when all values of $D(\omega T)$ lie on the linear section of the curve. Then the measured current varies linearly with $\overline{D(\omega T)}$, and the intersection of the straight sides may be obtained by analyzing $\overline{\theta(\omega T)}$.

In the ideal case when the alignment is perfect and the cavity modes are equal, the beam rotates about the center of the pinhole at a constant radius D so that the curve of Fig. 7 is followed exactly. Either misalignment or inequality of the modes shortens the linear section of the current peak, since equation (3) is valid only when all values of $D(\omega T)$ are on the linear section.

Suppose that the deflection is given by 3.2 (27):

$$\theta = \left\{\dot{\xi}^2(d)v^{-2} + \dot{\eta}^2(d)L^{-2}\right\}^{\frac{1}{2}}\omega^{-1}\left\{b_1^2 - (b_1^2 - b_2^2)\sin^2\omega T\right\}^{\frac{1}{2}}$$

Then

$$\bar{\theta} = \left\{\dot{\xi}^2(d)v^{-2} + \dot{\eta}^2(d)L^{-2}\right\}^{\frac{1}{2}}(2b_1/\omega\pi)E\left(\sqrt{1-(b_1/b_2)^2}\right)$$

Near resonance $\eta(d)$ is constant and $\left\{\dot{\xi}(d)/v\right\}$ is linear in V. Then the current peak is symmetric in V. The dependence upon V is the same as when $b_1 = b_2$, but the length of the sides is shortened, and the top of the peak is depressed. In a rather similar manner misalignment will not change the intersection of the sides but will affect

the resolution of the peak.

The R. F. tuning and the alignment are carefully adjusted so that the variation in $D(\omega T)$ is small and the linear section of the curve is efficiently utilized. By measuring the maximum current the beam may be centered on the pinhole with sufficient accuracy to obviate this source of difficulty.

IV. EXPERIMENTAL RESULTS AND THEIR INTERPRETATION

4.0 Procedure in Obtaining Data

For a year prior to the fall of 1954 Dr. Smythe and the author endeavored to increase the stability of various units to a point where decisive data could be collected. The elimination of one instability in several cases unmasked further problems. In the summer of 1954 it was discovered that the entrance holes in the flat end surfaces of the cavity were unaccountably not centered. With the correction of this condition the only remaining source of important instability was the charging of surfaces in the electron gun, and measurements were feasible if these surfaces were cleaned after every twenty hours of operating time.

Sufficient data were collected in the last quarter of 1954 to demonstrate the characteristics and limitations of the instrument. These data consisted of a series of determinations of the "resonant" voltages corresponding to a given length and frequency of the cavity. At least two measurements of each "resonant" voltage should be made in a day's operation in order that it be certain that the conditions in the electron gun remain unchanged.

The procedure in obtaining a series of current peaks will be summarized. The various filament and voltage supplies are brought into operating condition and allowed to stabilize. This usually requires at least an hour. The vacuum pressure is measured with an ion gauge, and the pressure is usually under 8×10^{-6} mm. of mercury.

With all units stable the electron beam is centered on the

collector pinhole by mechanical positioning of the collector, or by a small electrostatic deflection of the beam beyond the cavity. The current is maximized, thereby centering the collector and bringing the electron beam accelerating voltage close to resonance. The accelerating voltage may be set to every 0.1 volts by means of a Helipot, and each setting is reproducible to within 0.02 volts.

At the initial Helipot setting the accelerating voltage is measured by the standard megohm and potentiometer. The current passing through the collector pinhole is amplified and projected upon a 50 cm. galvanometer scale. This current reading and the corresponding Helipot setting are recorded. The R. F. pickup from the probes set in the cavity walls is also recorded. The accelerating voltage is changed to another value, and the Helipot setting, the received beam current, and the R. F. pickup reading are recorded. This procedure is repeated until the current peak is completed. The Helipot is then returned to its initial setting, any positional drift of the beam is investigated, and the accelerating voltage at this Helipot setting is again measured. The cavity frequency is measured both before and after every peak. It is sufficient reason to obviate a current peak if excessive variations occur in the R. F. frequency, the R. F. field intensity, the accelerating voltage supply, the intensity of the electron beam, or the position of the electron beam. This procedure is repeated until an adequate current peak at this "resonant" voltage is obtained.

It is desirable to obtain as many points as possible on the linear section of the current peak. However, if more points were obtained, the longer time required to complete the peak would

enhance the possibility of a variation in some critical element. Each peak would be more reliable, but fewer peaks would be collected. For this reason three or four points are collected on each linear section of the peak.

A current peak is obtained at each "resonant" voltage until a full set is collected. With the cavity length 1.1954 inches the "resonant" voltages were measured in the order 729, 1143, 2043, 729, 1143, 2043 volts. With the cavity length 1.6295 inches the order of measurement was 2129, 1357, 940, 2129, 1357, 940 volts.

These current peaks are plotted, and the intersection of the straight sides obtained. This intersection is obtained in terms of the Helipot setting. Knowledge of the voltage at the initial Helipot setting plus the reliable Helipot calibration yields the "resonant" voltage at the intersection.

Additional data are collected for each current peak: the ambient temperature, the resonant cavity temperature, the vacuum pressure, and the current zero on the galvanometer scale. Of these quantities only the cavity temperature affects the value of the "resonant" voltage. It is convenient in the analysis of data to correct the "resonant" voltage for the temperature variation. This correction has been obtained empirically for a cavity length of 1.6295 inches:

$$(\Delta V/V) = 3 \times 10^{-5} \Delta T \qquad (1)$$

where ΔT is in ^{o}C. This correction is due to the expansion of the molybdenum ring and to the bowing of the end surfaces. Taking the thermal coefficient of expansion of molybdenum as 5×10^{-6}, the cor-

rection for the cavity of length 1.1954 inches is:

$$(\Delta V/V) = 3.8 \times 10^{-5} \Delta T \qquad (2)$$

It is also convenient to correct the "resonant" voltage to the standard frequency, $f = 2.62000\ 10^9$ sec.$^{-1}$. This correction is obtained from

$$(\Delta V/V) = 2(\Delta f/f) \qquad (3)$$

Another factor affecting our resonances must be noted. In this laboratory there is a large magnet used with cloud chambers to investigate cosmic rays. When this magnet is in operation, it produces a stray field in the neighborhood of the instrument. This field may be as large as a gauss. Our shielding does not completely compensate for this field. The status of this magnet during each current peak is noted.

4.1 Characteristics of Current Peaks

The current peaks exhibit two straight sides when plotted against voltage. The extension of these straight sides produces an intersection that determines a "resonant" voltage. The width of these peaks with the current at one half its maximum value depends upon the cavity field strength. Typical values of these widths are tabulated below opposite the corresponding "resonant" voltage.

	"Resonant" Voltage	Width at Half Maximum
d = 1.1954 inches	2043 volts	13.0 volts
	1143 volts	5.5 volts
	729 volts	3.5 volts
d = 1.6295 inches	2129 volts	11.0 volts
	1357 volts	6.0 volts
	940 volts	3.3 volts

A clearer conception of these current peaks may be obtained by studying Fig. 8, where three peaks for a cavity length of 1.6295 inches are plotted. These peaks are typical and were obtained on December 13, 1954. They may be compared directly since the voltage and current scales are identical for all peaks. The fact that the middle peak has a larger beam current is not significant; this depends upon the focusing action of the electron gun. Often the gun is operated so that the current received increases with increasing voltage.

The resolution of these peaks is very good. Dr. Smythe and the author have independently determined seven "resonant" voltages from peaks taken on a typical day, and the results agreed within 0.01 volts on all but one peak, where the difference was 0.02 volts. While such agreement may be fortuitous, well formed peaks may be resolved to an estimated 0.03 volts and be assigned rigid confidence limits of $\pm$0.10 volts. Less certainty can be attached to peaks which are affected by drifts or fluctuations of the electron beam or cavity fields, but these peaks are useful as checks to the more accurate ones. It is of interest to calculate the standard deviation between two current peaks that are obtained consecutively for the same "resonant" voltage.

	"Resonant" Voltage	Deviation of Consecutive Peaks
d = 1.6295 in.	2129 volts	0.09 volts
	1357 volts	0.07 volts
	940 volts	0.04 volts
d = 1.1954 in.	2043 volts	0.11 volts
	1143 volts	0.11 volts
	729 volts	0.13 volts

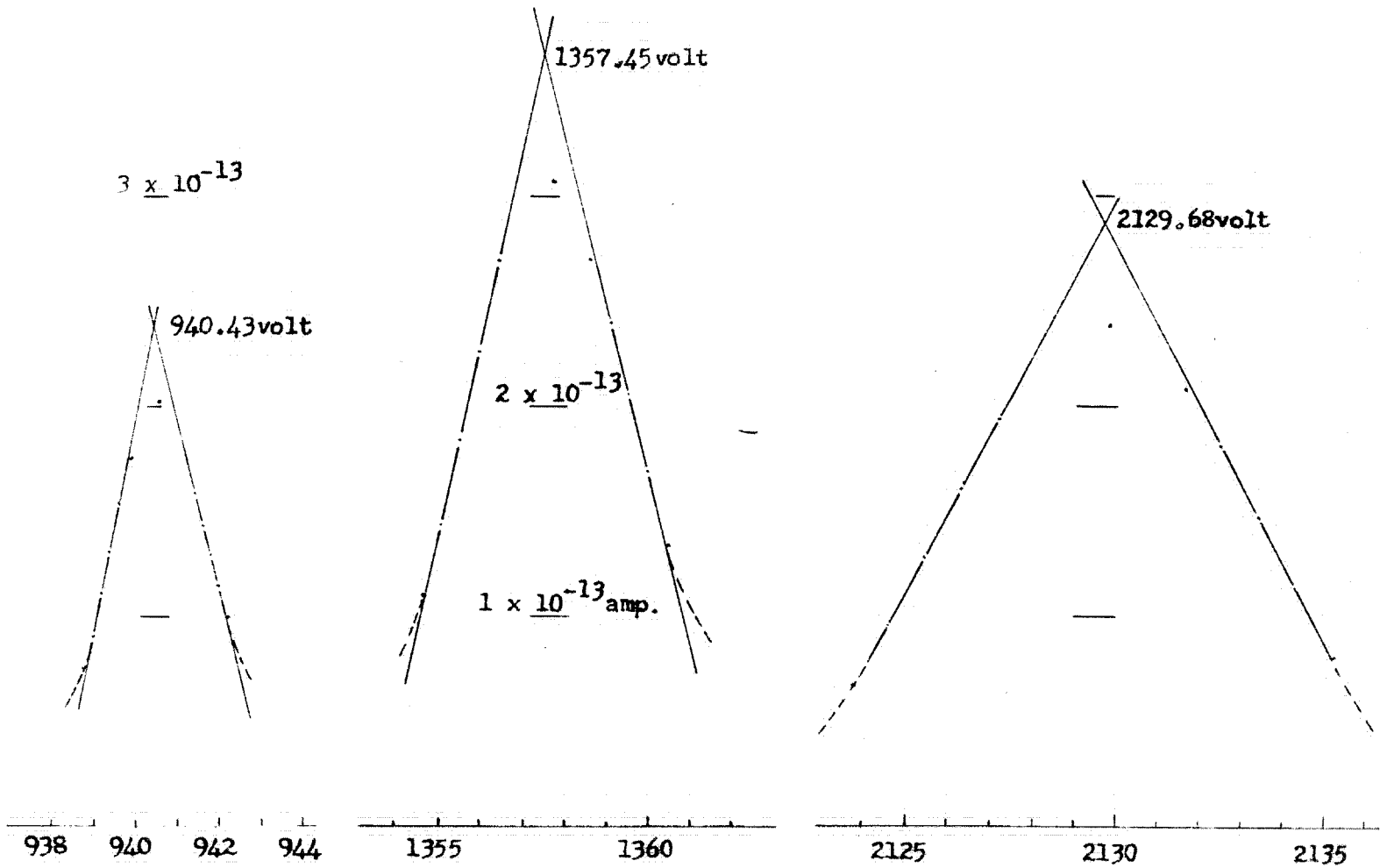

FIGURE 8. LONG CAVITY PEAKS.

Increased stability of the electron beam accounts for the smaller deviations for the longer cavity. In most cases one of the two consecutive measurements had appreciable drift or instability present. In view of these facts it is felt that a standard error of less than a tenth of a volt may be assigned to the determination of a "resonant" voltage from a current peak.

Theory predicts that these current peaks be essentially symmetric in voltage. The agreement of the experimental peaks with this prediction is only fair. The form of the current peaks corresponding to the 2043 and 2129 volt resonances agree well with theoretical predictions. However, current peaks for lower "resonant" voltages exhibit an asymmetry that becomes more marked as the "resonant" voltage decreases. This asymmetry is characterized by a shorter linear section and a decreased voltage sensitivity on the upper side of the peak. This effect is seen clearly in Fig. 9, which shows three current peaks obtained for a cavity length of 1.1954 inches on October 28, 1954. The voltage scale as measured from the "resonant" voltage is the same for the three peaks. The current zero is different for each peak, and the current scale has been normalized for convenience.

An asymmetric voltage spread of several volts in the electron beam would produce current peaks with this shape. This possibility has been investigated with a crossed-field velocity analyzer built by Dr. W. T. Ogier. It was found that the width of the voltage spread was less than 0.3 volts, which was the limit of the analyzer. Then the origin of these asymmetric current peaks must be in the resonant cavity.

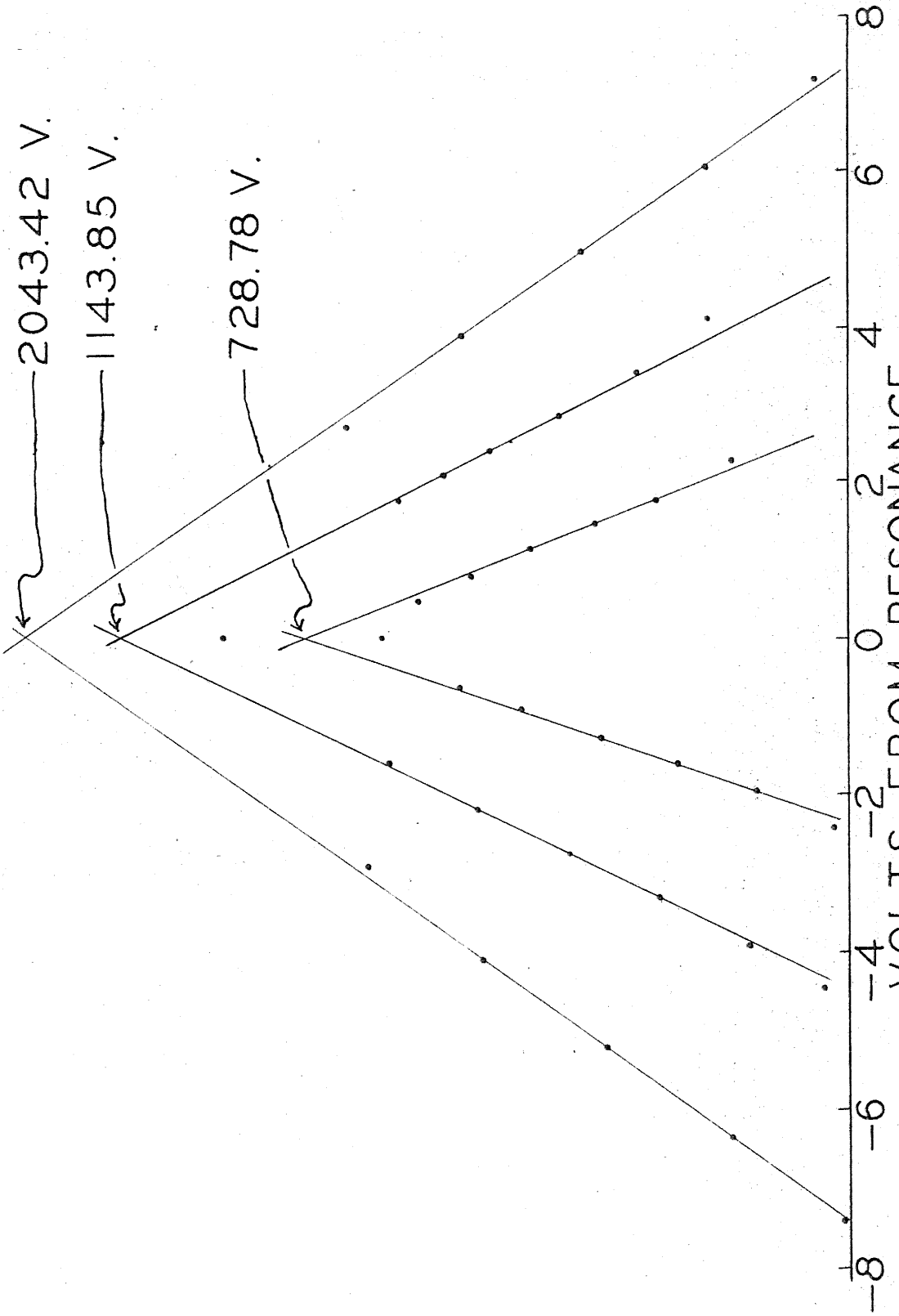

FIG. 9. SHORT CAVITY CURRENT PEAKS

The probable cause of the peak asymmetry is positive charging of the cavity near the entrance holes. The resulting defocusing fields would produce current peaks of this shape if sufficient charge accumulated. Other effects which would be produced by charging will appear and be discussed in later sections.

4.2 Determination of "Resonant" Voltages

In nineteen days spread through the last quarter of 1954 one hundred ten determinations of "resonant" voltage were obtained. The voltage obtained from each current peak was corrected to a cavity frequency of $2.62000\ 10^9$ sec.$^{-1}$ and a cavity temperature of 22.0°C. by means of equations 4.0(1), (2), and (3). If two or more peaks were obtained consecutively at one "resonant" voltage, a weighted mean was taken. In such cases the final current peak usually carried greater weight, since it was obtained under more stable operating conditions.

The determinations of the "resonant" voltages are tabulated in Table 1. The temporal order of the determinations in a day is obtained by reading from left to right, except on November 23, 1954, when reading must be from right to left. The presence or absence of an asterisk (*) by a determination indicates that the magnet used in cosmic ray investigations was operating or not. The magnet was in operation during all measurements performed with the longer cavity.

Some of the values listed may be in error due to difficulties in resolving the current peaks, but most are the correct "resonant" voltage determined by the intersection of the current peaks within

Table 1. "Resonant" Voltage Determinations

d=1.1954 in. f=2.62000 10^9 sec.$^{-1}$ Cavity Temp.=22.0°C.

Date	n=5	n=4	n=3	n=5	n=4	n=3
9/20/54	729.59	1144.02	2043.52	730.11	1144.19	
9/29/54	730.54	1144.18	2044.09	730.48	1144.16	2043.98
	730.40					
10/2/54	730.17	1144.51	2044.00	729.78	1144.27	2043.53
10/12/54	729.26	1144.10	2043.86	729.86	1143.77*	2043.12*
10/13/54	729.56	1144.14	2043.05*	728.94*	1143.79*	2043.05*
10/19/54	729.29	1144.08	2043.72	729.66	1144.12	2043.73
10/20/54	729.59	1144.02	2043.93	729.43	1144.25	2043.84
10/27/54	728.57*	1143.25*	2042.70*	729.23*	1143.29*	2042.83*
10/28/54	731.81*	1143.84*	2043.42*	728.78*	1143.85*	2043.29*
11/2/54	731.31*	1143.91*	2043.02*	728.84*	1144.14*	2042.63*
11/8/54	731.91*	1143.79*	2043.32*	728.66*	1143.55*	2042.99*
	728.45*					
11/23/54	729.22*	1143.88*	2043.13*	728.91*	1143.05*	2043.26*

d=1.6295 in. f=2.62000 10^9 sec.$^{-1}$ Cavity Temp.=22.0°C.

Date	n=4	n=5	n=6	n=4	n=5	n=6
12/8/54	2130.33*	1357.38*	940.55*	2129.65*	1357.34*	940.74*
12/10/54	2129.97*	1357.27*	940.54*	2129.42*	1357.49*	940.42*
12/13/54	2129.57*	1357.41*	940.41*	2129.57*	1357.40*	940.40*
12/14/54	2129.90*	1357.39*	940.39*	2129.62*	1357.45*	940.43*
12/15/54	2129.89*	1357.30*	940.55*	2129.64*	1357.57*	940.46*
12/24/54	2129.76*	1357.28*	940.74*	2130.20*	1357.34*	940.47*
12/31/54		1357.89*				

0.1 volts. Then the fluctuations in the listed values represent real shifts in the "resonant" voltage. If these fluctuations are random about the true "resonant" voltage, the mean values obtained will enable us to calculate (e/m_o). It will be seen that this assumption is not valid, and an explanation for the phenomena will be offered.

The variation in values obtained for the longer cavity is small, and their character appears random. The data may be analyzed in two ways. Each determination may be considered a datum, and each "resonant" voltage obtained as the mean of twelve determinations. Then:

$V(n=4)=2129.79\pm0.08$ volts

$V(n=5)=1357.39\pm0.03$ volts

$V(n=6)=940.49\pm0.04$ volts

$V(n=4)-V(n=5)=772.40\pm0.09$ volts

$V(n=5)-V(n=6)=416.90\pm0.05$ volts

where the quoted error is the standard error of the mean, assuming random fluctuations.

Another method of analysis is to consider the voltage differences between consecutive "resonant" voltage determinations as data. This method has greater theoretical justification, but the results are essentially the same as above.

$V(n=4)-V(n=5) = 772.44\pm0.09$ volts

$V(n=5)-V(n=6) = 416.83\pm0.06$ volts

These values may be taken as the peak differences in the longer cavity.

The data obtained for the shorter cavity are complicated by larger variations that in some cases are certainly not random. The first peaks measured on October 28, November 2, and November

2, and November 8 are clearly not random fluctuations. These peaks will be neglected in the statistical analysis and discussed later. Those peaks obtained with the magnet in operation must be differentiated from the remainder. The individual "resonant" voltages are certainly affected by the magnet, although it is not certain that the voltage differences are.

The system of statistical analysis does not affect the mean values obtained. The results obtained for "resonant" voltages when the magnet is in operation are:

$V(n=3)=2043.06\pm0.07$ volts
$V(n=4)=1143.68\pm0.09$ volts
$V(n=5)=728.84\pm0.10$ volts

$V(n=3)-V(n=4)=899.38\pm0.11$ volts
$V(n=4)-V(n=5)=414.84\pm0.14$ volts

The "resonant" voltages when the magnet is not in operation are:

$V(n=3)=2043.82\pm0.06$ volts
$V(n=4)=1144.17\pm0.04$ volts
$V(n=5)=729.84\pm0.12$ volts

$V(n=3)-V(n=4)=899.65\pm0.07$ volts
$V(n=4)-V(n=5)=414.34\pm0.13$ volts

4.3 Interpretation of Results

The feasibility of obtaining a value of (e/m_o) from this data will be considered. The impossibility of a meaningful calculation is best seen in the following manner. From the energy equation

$$(e/m_o)V_n=\tfrac{1}{2}(f/n)^2(d+\Delta d)^2R_n \qquad (1)$$

where R_n is the relativistic correction

$$R_n=1+(3/2)(eV_n/m_oc^2)+1/4\,(eV_n/m_oc^2)^2\ldots \qquad (2)$$

we obtain, when Δd is independent of velocity:

$$\frac{V_k - V_1}{V_1 - V_m} = (1/k)^2 (R_k/R_1) \frac{1-(k/1)^2(R_1/R_k)}{1-(1/m)^2(R_m/R_1)} \qquad (3)$$

If R_k, R_1, and R_m are evaluated from the measured "resonant" voltages, it may be shown that the right-hand side of equation (3) is essentially independent of contact potentials in the electron gun and insensitive to the value of (e/m_o). From the data of the last section, the right-hand side of equation (3) is

$$\frac{V_3 - V_4}{V_4 - V_5} = 2.1688 \text{ when } d=1.1954"; \quad \frac{V_4 - V_5}{V_5 - V_6} = 1.8476 \text{ when } d=1.6295"$$

The left side of equation (3) is

$$\frac{V_3 - V_4}{V_4 - V_5} = 2.1680 \text{ when } d=1.1954"; \quad \frac{V_4 - V_5}{V_5 - V_6} = 1.8527 \text{ when } d=1.6295"$$

The differences between the right and left-hand sides of equation (3) are -0.04% for the short cavity and + 0.28% for the long cavity. Equation (3) was derived on the assumption that the effective length of the cavity was independent of voltage.

It follows that the effective length of the long cavity varies over the three resonances by an amount corresponding to several volts. Neglecting other factors, this variation in itself would prevent an accurate determination of (e/m_o). The fact that the differences between the two sides of equation (3) are opposite in sign for the short and long cavities indicates a basic incompatibility between the two sets of data. Detailed analysis verifies this.

Investigation has demonstrated that the origin of these inconsistencies must lie in the resonant cavity. The hypothesis that

the cavity walls become positively charged fits all the facts. No other hypothesis either explains all the facts, or, indeed, appears as likely.

It is known as a fact that oil films from the pump oil form on all surfaces in the system. Continuous cold trapping does not prevent this from occurring. When the cavity was dismantled to insert the molybdenum spacer ring, these films were observed visually. The surfaces were cleaned before the insertion of the ring. The potential reached by an oil film on a conducting surface is the product of the thickness of the film times the field intensity in the film. This field is either determined by the breakdown potential of the film, or by the rates of charging and leaking. The latter is more likely in this experiment. Even very thin films, invisible to the eye, may attain appreciable potentials.

Only one mechanism of charging of the cavity surfaces appears likely. The geometry of the cavity prevents the electron beam from impinging on any cavity surface, and gas ions formed are too massive to be affected by the R. F. fields. Since the "resonant" voltages are independent of the vacuum pressure, little charging can occur from ionized or scattered particles. The region surrounding the exit pinhole of the cavity is the origin of soft X-rays due to the electron beam falling on this surface. These soft X-rays fall upon the plane surface surrounding the entrance hole in the opposite cavity wall and upon the interior of the near circular entrance hole. These X-rays can "knock out" many electrons from both the chromium and the oil film, leaving a positive charge on this film.

The charge accumulated in this manner and the rate of charging, will depend upon the beam intensity and the beam voltage. The exact effect of a positively charged surface upon the measured "resonance" will depend upon the configuration of the fields. However, the electrons are accelerated in the cavity so that a lesser accelerating voltage in the electron gun may be applied to attain "resonance". The measured "resonant" voltage will be decreased as the positive charging increases.

If the oil film is not too dense, if the beam intensities used are approximately the same, and if the charge is first brought to equilibrium by use of a high voltage beam, the fluctuations should not be large. This is the case with the measurements performed with the longer cavity. The charge acquired by the two thousand volt beam is not dissipated immediately, and the subsequent lower voltage resonances are depressed. All of the twelve determinations of the 1357 volt resonance obtained subsequent to a 2130 volt resonance, have a mean of 1357.39 ± 0.03 volts. All twelve determinations of this resonance with no prior higher voltage measurements have a mean of 1357.89 ± 0.02. The closest values in the different sets are 0.27 volts apart. This effect also accounts for the direction of the difference noted in equation (3).

This effect is also apparent in the shorter cavity. Consider the 730 volt resonances from October 27 to November 23. All determinations taken after a higher voltage resonance are near 729 volts, while those taken before the application of a higher voltage beam are above 731 volts. The first determination of October 27 appears to be an exception, but the beam had previously been raised

to 2000 volts to check on current intensities. It is believed that this effect became so prominent because of increased thickness of the oil film, and that it was not apparent on October 19 and October 20, because the electron beam was in operation for an hour longer than usual before the first measurement was made.

Charging of the cavity also explains the variation of the "resonant" voltage with stray magnetic field. With the different trajectories of the electrons the X-rays will originate in a different area so that the measured voltage will be different.

The increased fluctuations of the values obtained with the magnet in operation is also considered due to the thicker oil film, since these measurements were principally taken subsequent to those made with the magnet off. At any rate the values obtained with the magnet in operation on October 12 and October 13 agree with one another very well.

No correction can be applied to the data to obtain (e/m_o), and no simple change in the design of the equipment can adequately prevent the charging of these oil films.

4.4 Conclusions

The data obtained in this experiment were not adequate to obtain a significant value of (e/m_o). The inadequacy of the data was primarily due to: 1) the formation of oil films upon the cavity walls; 2) the incidence of soft X-rays upon the cavity surfaces, originating from about the exit pinhole; 3) insufficient magnetic shielding.

Other important difficulties that hampered measurements were: 1) the formation and charging of non-conducting deposits

on the electrodes of the electron gun; 2) deviation of the resonant cavity from an ideal shape; 3) the high stability required of all elements.

With one exception all of these obstacles could have been surmounted. The decisive handicap was the use of oil diffusion pumping to secure a vacuum. It is significant that the preliminary experiment, performed by Dr. Wilts[11] in a small mercury pumped system, did not encounter the described difficulties. The inability to prevent the formation of oil films in an oil pumped system was not generally known at the time this experiment was originated. The construction of the main vacuum envelope from aluminum prohibits mercury pumping.

An accurate determination of the specific charge of an unbound electron remains highly desirable. The method of measurement used in this experiment possesses several important virtues: 1) the relative ease in accurate determinations of length, frequency, and voltage; 2) the elimination of error arising from contact potentials in the electron source; 3) the excellent resolution of the current peaks; 4) the elimination of consistent error due to charged surfaces other than in the resonant cavity, where the sensitivity is not large; 5) the rapidity in the collection of data, if oil films are not present.

The first two advantages listed above are proven. The last three are believed to be correct in a mercury pumped system. The resolution of the current peaks is very good under existing conditions, and should be excellent for a peak symmetric in voltage and uninfluenced by charged surfaces. To fulfill the fourth advantage the resonant cavity should be composed of a suitable material and mercury pumped. The electron beam should be prevented from impinging

upon any cavity surface, and a shield placed about the cavity exit pinhole to prevent X-rays from striking the cavity walls. Under these precautions the surface charging should be negligible. The design of the electron gun used in this experiment is quite satisfactory. If the electrode surfaces did not require periodic cleaning, the data collected in three months could have been obtained in a single month.

These advantages indicate that an experimenter, who profits from the lessons in this paper, could use this method to perform a significant measurement of (e/m_o). In addition to the measures taken to prevent charging in the cavity his design would have to include better magnetic shielding so that the effects of external magnetic fields would be eliminated. This shielding should be outside the vacuum system to facilitate pumping. The cost of this shielding would probably be the largest single expense of the experiment.

The electron gun, the current detection system, the measuring equipment, and the power supplies used in this experiment are adequate for a significant measurement. Resolution of the current peaks requires that the vacuum envelope must be approximately as long as the one used in this experiment.

The beam collimation used in this experiment is nearly ideal. A wider beam causes loss in resolution, while a narrower beam with geometric trajectories is very difficult to obtain. No large improvement could be obtained by a change of the cavity characteristics. A longer cavity or a more intense magnetic field will not achieve significant improvement of resolution, since the beam displacement will compete with beam deflection. The frequency of the

cavity may be increased somewhat, but the radius of the cavity must not be too small, or the effects of the probes in the cavity walls will be too large at the cavity axis. One improvement suggested by this experiment would be to construct the plane surfaces of the cavity from a single material, rather than to use plating.

It is believed that an experiment, that combines these design improvements with an empirical determination of the end hole correction, possibly for three cavity lengths, should be capable of a determination of (e/m_o) to nearly 10 ppm.

APPENDIX I.

R. F. Fields in Cavity with Deformed Cylindrical Wall

A resonant cavity bounded by the surfaces

$$\rho = b, \quad \begin{cases} \pi \geqslant \phi \geqslant \Delta\phi \\ -\pi \leqslant \phi \leqslant -\Delta\phi \end{cases} \quad ; \quad \rho = b - \epsilon, \quad -\Delta\phi \leqslant \phi \leqslant \Delta\phi$$

$$z = \frac{d}{2} \qquad\qquad z = -\frac{d}{2}$$

is operated in the TM_{110} mode. When $\epsilon = 0$, the vector potential of a single mode is

$$\underset{\sim}{A} = -\underset{\sim}{k}(2C/\beta_o)J_1(\beta_o\rho)\sin(\phi+\psi)\cos(\omega t)$$

where $\beta_o b = (\omega b/c) = 3.8317$. Since ψ may take on any value, the above expression represents two orthogonal, degenerate modes. The degeneracy disappears when $\epsilon > 0$, and we may write the vector potentials of the two orthogonal modes as

$$\underset{\sim}{A}_1 = \underset{\sim}{k}(2/\beta_1)\left\{ C_1 J_1(\beta_1\rho)\cos\phi + C_o J_o(\beta_1\rho) + \sum_{n=2}^{\infty} C_n J_n(\beta_1\rho)\cos n\phi \right\}\cos\omega t$$

$$\underset{\sim}{A}_2 = \underset{\sim}{k}(2/\beta_2)\sum_{n=1}^{\infty} D_n J_n(\beta_2\rho)\sin(n\phi)\cos\omega t.$$

These expressions satisfy the boundary conditions on the surfaces $z = d/2$, $z = -d/2$. The vector potential must vanish on the remaining surfaces. To obtain the boundary conditions in the proper form for a perturbation calculation we define the vector potential in the region $0 \leqslant \rho \leqslant b$ for all ϕ, and the boundary conditions for the first mode become:

$$A_z(\rho=b) = \begin{cases} 0; & \pi \geqslant |\phi| \geqslant \Delta\phi \\ (2/\beta_1)\sum_{n=0}^{\infty} C_n\left[J_n(\beta_1 b) - J_n(\beta_1 b - \beta_1\epsilon)\right]\cos(n\phi)\cos\omega t & -\Delta\phi \leqslant \phi \leqslant \Delta\phi \end{cases}$$

Utilizing the orthogonality of the trigonometric terms we obtain the equations

$$\pi(1+\delta_s^o)J_s(\beta_1 b)C_s = \left[J_s(\beta_1 b)-J_s(\beta_1 b-\beta_1\epsilon)\right]\left\{2\Delta\phi+(1-\delta_s^o)\frac{\sin 2s\Delta\phi}{s}\right\}C_s$$

$$+\sum_{n=0}^{\infty}{}' C_n(1-\delta_s^n)\left[J_n(\beta_1 b)-J_n(\beta_1 b-\beta_1\epsilon)\right]\left\{\frac{\sin(n-s)\Delta\phi}{n-s}+\frac{\sin(n+s)\Delta\phi}{n+s}\right\}$$

Application of standard perturbation techniques yields a solution correct to order (ϵ/b)

$$\underset{\sim}{A}_1 = \underset{\sim}{k}(2C_1/\beta_1)\sum_{n=o}^{\infty}{}' (C_n/C_1)J_n(\beta_1\rho)\cos(n\phi)\cos(\omega t)$$

where

$$(C_n/C_1) = \frac{(\beta_o b)J_1'(\beta_o b)}{(1+\delta_n^o)\pi J_n(\beta_o b)}\ (\epsilon/b)\left\{\frac{\sin(n-1)\Delta\phi}{n-1}+\frac{\sin(n+1)\Delta\phi}{n+1}\right\}$$

for $n = 0, 2, 3, 4, 5, \ldots$

and $\beta_1 = \beta_o\left\{1+(\epsilon/\pi b)(\Delta\phi+\tfrac{1}{2}\sin 2\Delta\phi)\ \ldots\right\}$

The same techniques yield as the solution of the second mode

$$\underset{\sim}{A}_2 = \underset{\sim}{k}(2D_1/\beta_2)\sum_{n=1}^{\infty}{}' (D_n/D_1)J_n(\beta_2\rho)\sin(n\phi)\cos(\omega t)$$

where

$$(D_n/D_1) = \frac{(\beta_o b)J_1'(\beta_o b)}{\pi J_n(\beta_o b)}\ (\epsilon/b)\left\{\frac{\sin(n-1)\Delta\phi}{n-1}-\frac{\sin(n+1)\Delta\phi}{n+1}\right\}$$

for $n = 2, 3, 4, 5, \ldots$

and $\beta_2 = \beta_o\left\{1+(\epsilon/\pi b)(\Delta\phi-\tfrac{1}{2}\sin 2\Delta\phi)\ \ldots.\right\}$

We are interested in the fields near the cavity axis, which are derived from the leading terms in the above expansions. In

the expansion about the cavity axis all perturbation terms of quadratic and higher order in x and y are omitted since they are negligible. Then near the cavity axis the fields are

$$\underset{\sim}{A}_1 = \underset{\sim}{k}C_1\left\{x+(2\epsilon/\pi)\sin(\Delta\phi)\ldots\right\}\cos(\omega t)$$

$$\underset{\sim}{B}_1 = -C_1\underset{\sim}{i}\left\{(\beta_1{}^2xy/4)+(\beta_o{}^2\epsilon y/2\pi)(\sin\Delta\phi-(1/3)\sin3\Delta\phi)\ldots\right\}\cos\omega t$$

$$-C_1\underset{\sim}{j}\left\{1-\beta_o{}^2\epsilon x(3\sin\Delta\phi+(1/3)\sin3\Delta\phi)/2\pi-\beta_1{}^2(3x^2+y^2)/8\ldots\right\}\cos\omega t$$

$$\underset{\sim}{A}_2 = \underset{\sim}{k}D_1\left\{y\ \ldots\right\}\cos(\omega t)$$

$$\underset{\sim}{B}_2 = D_1\underset{\sim}{i}\left\{1-\beta_o{}^2\epsilon x(\sin\Delta\phi-(1/3)\sin3\Delta\phi)/2\pi-\beta_2{}^2(3y^2+x^2)/8\ldots\right\}\cos\omega t$$

$$+\ D_1\underset{\sim}{j}\left\{\beta_2{}^2xy/4+\beta_o{}^2\epsilon y(\sin\Delta\phi-(1/3)\sin3\Delta\phi)/2\pi\ldots\right\}\cos\omega t$$

In this experiment $\Delta\phi \leq 1/8$, and we may allow $\sin(\Delta\phi)\approx\Delta\phi$ and $\sin(3\Delta\phi)\approx 3\Delta\phi$. Moreover the change in the volume of the cavity is $\delta v = 2bd\epsilon\Delta\phi$, and the cavity volume is $\pi b^2 d$. We may write

$$\underset{\sim}{A}_1 = \underset{\sim}{k}C_1\left\{x+b(\delta v/v)\ldots\right\}\cos\omega t$$

$$\underset{\sim}{B}_1 = -C_1\left\{\underset{\sim}{i}(\beta_1{}^2xy/4)+\underset{\sim}{j}\left[1-\beta_o{}^2bx(\delta v/v)-\beta_1{}^2(3x^2+y^2)/8\ldots\right]\right\}\cos(\omega t)$$

$$\underset{\sim}{A}_2 = \underset{\sim}{k}D_1 y\cos(\omega t)$$

$$\underset{\sim}{B}_2 = D_1\left\{\underset{\sim}{i}\left[1-\beta_2{}^2(3y^2+x^2)/8\ldots\right]+\underset{\sim}{j}(\beta_2{}^2xy/4)\right\}\cos(\omega t)$$

$\underset{\sim}{A}_2$ and $\underset{\sim}{B}_2$ are not appreciably affected by the deformation of the cavity. Then only the mode, whose tangential magnetic field does not vanish at the center of the deformation, is altered.

The deformation treated here has no dependence upon z.

The circular holes in the cylindrical surface of the cavity used in this experiment produce perturbation terms that are z dependent. The discrepancy between the more accurate z dependent solutions and the z independent solutions above is not significant for this experiment.

APPENDIX II.

Form of First Order Resonance Condition

There exist two cavities with lengths, d_1 and d_2, which have a resonance for the same velocity, v. The equations to be solved are 3.2 (17):

$$\int_{-d_1}^{o} \left\{F_1(z)\cos(\omega z/v)-(\omega/v)G_1(z)\sin(\omega z/v)\right\} d(\omega z/v) = 0 \qquad (1)$$

$$\int_{-d_2}^{o} \left\{F_2(z)\cos(\omega z/v)-(\omega/v)G_2(z)\sin(\omega z/v)\right\} d(\omega z/v) = 0 \qquad (2)$$

under the conditions of 3.1 (9) and (10):

$$F_1(u-\tfrac{1}{2}d_1)=F_2(u-\tfrac{1}{2}d_2)\ ;\ G_1(u-\tfrac{1}{2}d_1)=G_2(u-\tfrac{1}{2}d_2) \quad -\tfrac{1}{2}d_1 \leqslant u \leqslant \tfrac{1}{2}d_1$$

$$F_2(u-\tfrac{1}{2}d_2)=G_2(u-\tfrac{1}{2}d_2)=0 \qquad u \leqslant -\tfrac{1}{2}d_1 \qquad (3)$$

$$F_2(u-\tfrac{1}{2}d_2)=1\ ;\ G_2(u-\tfrac{1}{2}d_2)=0 \qquad u \geqslant \tfrac{1}{2}d_1$$

Then if we substitute $z = u-\frac{1}{2}d_1$, $z=u-\frac{1}{2}d_2$, in equations (1) and (2) respectively, and if we define

$$I = \int_{-\frac{1}{2}d_1}^{+\frac{1}{2}d_1} \left\{F_1(u-\tfrac{1}{2}d_1)\cos(\omega u/v)-(\omega/v)G_1(u-\tfrac{1}{2}d_1)\sin(\omega u/v)\right\} d(\omega u/v) \qquad (4)$$

$$J = \int_{-\frac{1}{2}d_1}^{+\frac{1}{2}d_1} \left\{F_2(u-\tfrac{1}{2}d_1)\sin(\omega u/v)+(\omega/v)G_1(u-\tfrac{1}{2}d_1)\cos(\omega u/v)\right\} d(\omega u/v) \qquad (5)$$

we obtain

$$I\cos(\omega d_1/2v)+J\sin(\omega d_1/2v) = 0 \qquad (6)$$

$$\left\{I-\sin(\omega d_1/2v)\right\}\cos(\omega d_2/2v)+\left\{J+\cos(\omega d_1/2v)\right\}\sin(\omega d_2/2v)=0 \qquad (7)$$

Subtracting and adding $\sin(\omega d_1/2v)\cos(\omega d_1/2v)$ to equation (6):

$$\left\{I-\sin(\omega d_1/2v)\right\}\cos(\omega d_1/2v)+\left\{J+\cos(\omega d_1/2v)\right\}\sin(\omega d_1/2v) = 0 \qquad (8)$$

Both terms contained in brackets in equations (7) and (8) do not vanish. This may be verified by substitution of a simple trial value of $F(z)$ and $G(z)$. Then from (7) and (8)

$$\tan(\omega d_1/2v) = \tan(\omega d_2/2v) = f(\omega/v) \qquad (9)$$

or

$$(\omega d_1/2v) = n\pi+\tan^{-1}f(\omega/v) \qquad (10)$$

This may be written, remembering ω is a constant in this experiment,

$$(\omega/v)(d_1+\Delta d(v)) = 2n\pi \qquad (11)$$

REFERENCES

1. J. W. DuMond and E. R. Cohen

   Rev. Mod. Phys. 20 82 (1948)

2. J. W. DuMond and E. R. Cohen

   Rev. Mod. Phys. 25 691 (1953)

3. F. G. Dunnington

   Phys. Rev. 52 475 (1937)

4. S. H. Koenig, A. G. Prodell, and P. Kusch

   Phys. Rev. 88 191 (1952)

5. R. Beringer and M. Heald

   Phys. Rev. 95 1474 (1954)

6. R. Karplus and N. Kroll

   Phys. Rev. 77 536 (1950)

7. Thomas, Driscoll, and Hipple

   Phys. Rev. 78 787 (1950)

8. W. R. Smythe

   Static and Dynamic Electricity, McGraw-Hill (1950) p. 535

9. W. T. Ogier

   Doctorate Thesis, C.I.T. (1953)

10. G. C. Dacey

    Doctorate Thesis, C.I.T. (1951)

11. C. H. Wilts

    Doctorate Thesis, C.I.T. (1948)

12. G. L. Felt

    Doctorate Thesis, C.I.T. (1951)

13. J. N. Harris

    Rev. Sci. Inst. 23 409 (1952)

14. W. R. Smythe

Static and Dynamic Electricity, McGraw-Hill (1950) pp. 531, 535

15. W. R. Smythe

J. Appl. Phys. 23 447 (1952)